NANOPETROPHYSICS OF THE UTICA SHALE,

APPALACHIAN BASIN,

OHIO, USA

by

OKWUOSA FRANCIS CHUKWUMA

Presented to the Faculty of the Graduate School of

The University of Texas at Arlington in Partial Fulfillment

of the Requirements

for the Degree of

MASTER OF SCIENCE IN EARTH AND ENVIRONMENTAL SCIENCE

THE UNIVERSITY OF TEXAS AT ARLINGTON

May 2015

Abstract

NANOPETROPHYSICS OF THE UTICA SHALE,

APPALACHIAN BASIN,

OHIO, USA

Okwuosa Francis Chukwuma, M.S

The University of Texas at Arlington, 2015

Supervising Professor: Q.H Hu

The introduction of horizontal drilling combined with the ability to perform multiple-stage hydraulic fracture treatment has enabled the oil and gas industry to explore previously un-exploitable source formations, where it is estimated that 85% of the original reserves still resides. The application of these techniques provides economic gas and oil flow in extremely low porosity and permeability reservoirs. The Utica play, like the Bakken, Eagle ford, Marcellus, Haynesville, Permian and Niobrara plays are the current focus for unconventional reservoir exploration in the United States where it is estimated that shale gas and oil production from these plays would reach 80 billion cubic feet per day and 9.6 million barrels per day, respectively, by the year 2020 (EIA, 2014).

However, despite these recent advances in production techniques used in stimulating tight shale reservoirs, most shale wells are still characterized by overall low recovery and steady steep decline in production typical to unconventional plays. The Utica Shale is not excluded from this, with production from this play showing an initial decline rate of 65% after its first year of production. This may be as a result of the low pore connectivity and very narrow pores that affects movement of hydrocarbon from the shale matrix to the wellbore. A number of factors such as pressure volume and temperature (pvt),

pore grain composition, multiphase fluid flow have been attributed to this observed phenomenon in shale reservoirs. However, researchers have not investigated the pore structure of the nanopores storing and transporting hydrocarbon.

This study will evaluate pore-size distribution and pore connectivity of Utica Shale samples obtained from J. Goins (GS-3), Prudential (1-A) and Fred Barth (#3) wells in Ohio. Using mercury intrusion porosimetry, fluid (DI water, API brine and n-decane) and tracer imbibition, and edge-only accessible porosity tests, we were able to investigate the pore structure, edge accessible porosity, and the degree to which wettability is associated with mineral and organic kerogen phases. The MICP tests gave us initial sample characterization of basic petrophysical properties (porosity, permeability, pore-size distribution, and tortuosity). We examined imbibition behavior and imbibed tracer distribution for fluids (API brine or n-decane) to examine the association of tracers with mineral or kerogen phases using LA-ICP-MS mapping to measure the presence of tracers in each fluid.

Mercury intrusion capillary pressure analyses shows that the Utica pores are predominantly in the nanometer size range, with measured average pore-throat diameter of 4 nm to 6 nm across the study location. Imbibition slopes shows an evidence of low pore connectivity which is consistent with percolation theory interpretation of low connectivity and may be due to the observed small pore-throat distribution. These innovative approaches are significant because they may hold the key to understanding fluid flow and pore structure in the nanopores by stipulating the limited accessibility and connectivity in the Utica Shale.

Table of Contents

List of Illustrations

List of Tables

Chapter 1

Introduction

Historically, shale has been looked upon by petroleum geologist as an impermeable source or seal rock that serve to feed or trap hydrocarbons found in more permeable sandstone or limestone reservoirs. Conventional oil and gas exploration has targeted sandstone or limestone formations for this reason. However, with an increased demand for energy, the advent of horizontal drilling combined with the ability to perform multiple-stage fracture treatments have resolved the impermeability problem, enabling organically rich shale formations to produce hydrocarbon in commercial quantity. This is particularly true in the United States, where numerous shale plays such as the Barnett, Utica, Eagle Ford, Marcellus and others are currently being produced (Figure 1-1). Such unconventional resources include shale gas and liquids, tight gas and oil (low-permeability), and coalbed methane (Thomas et al., 2012). As opportunities for exploiting conventional resources are becoming more limited, focus is now on unconventional resources to meet the ever growing demand of energy, particularly in the United States.

Production of natural gas and oil from shale and other tight resources in the U.S has significantly increased, with seven oil and gas shale plays (Figure 1-1) accounting for nearly 95% of domestic tight oil production growth and virtually all natural gas production in the past few years (EIA, 2015). The Energy Information Administration (EIA) estimates that shale gas and oil production is expected to reach 80 billion cubic feet per day and 9.6 million barrels per day, respectively, by the year 2020 (EIA, 2014).

However, despite the increasing gas and oil production from shale formations, proponents of the so-called 'shale revolution' argue that it would be difficult to sustain. Analysis of data from 65,000 shale wells in 30 shale-gas and 21 tight-oil in the U.S. led Hughes (2013; 2014), to state the following points on shale gas and tight oil

1

On shale gas, Hughes claims:

- High productivity shale gas plays are not ubiquitous: just six plays account for 88% of total production, several of which are in decline.

- Individual well decline rates ranges from 80% to 95% after 36 months in the top six U.S. plays.

- Overall field declines requires 30% to 50% of production to be replaced annually with more drilling – roughly 7000 wells a year simply to maintain production.

- Dry shale gas plays require $42 billion/year in capital investment to offset declines.

On tight oil Hughes states the following points

- More than 80% of tight oil production is from two unique plays: the Bakken and the Eagle Ford.

- Well decline rates are steep – between 50% and 80% in the first year

- Overall field decline rates are such that 40% of production must be replaced annually to maintain production.

Baihly et al. (2011) and Maugeri (2013) – studied the decline rate in wells located at major shale plays (Barnett, Fayetteville, Woodford, and Haynesville). All four plays showed similar decline trend usually after the first year of production. While this steep decline and low overall recovery in shale plays are widely acknowledged in the oil and gas industry, investigations into their root cause(s) are surprisingly low (Hu and Ewing, 2014).
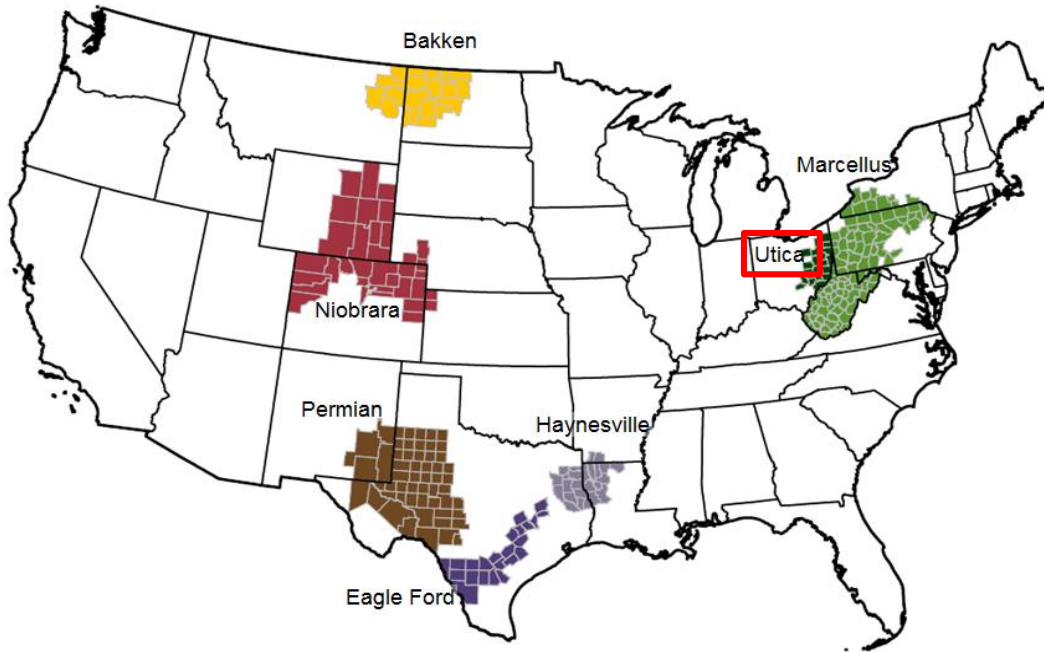
Figure 1-1 Major oil and natural gas production region: Seven shale plays account for 95% of domestic oil production growth and all domestic natural gas production growth through 2011 – 2013. (EIA, 2015).

Utica Shale

Extending through much of the regions of the Appalachian basin in the U.S. and Canada, the Utica/Point Pleasant Shale (referred herein as the Utica Shale) is an organic and clay-rich, calcareous black shale that was deposited during the Late Ordovician (Ryder, 2006). The U.S Geological Survey (USGS) assessment of undiscovered technically, recoverable oil and gas resources report (Ryder, 2008), identified the Utica Shale and Late Ordovician age equivalents in the Utica-Lower Paleozoic Total Petroleum System (TPS), as the primary source rock for multiple lower Paleozoic sandstone and carbonate units that are important reservoirs (Ryder, 2008; Kirschbaum et al., 2012). The Utica shale covers approximately 170,000 mi^2 of the Appalachian basin from northern Tennessee to southeastern New York and from central Ohio to eastern West Virginia. Like

3

the Marcellus play above it, The Utica Shale has the potential to become an enormous natural gas and tight oil resources (Figure 1-2) due to its vast amount of natural gas liquid and crude oil (Swift el al., 2014). The US Energy Information Administration (EIA) in 2012 estimated that the Utica Shale in the U.S held 15.712 TCF of unproved, technically recoverable gas with average well Estimated Ultimate Recovery being 1.13 BCF of gas (EIA, 2012). The USGS also assessed technically recoverable (unconventional) oil and gas resources for the Utica Shale of the Appalachian basin province, resulting in estimated means of 940 MMBO, 38.2 TCFG, and 208 MMBNGL (USGS, 2012).
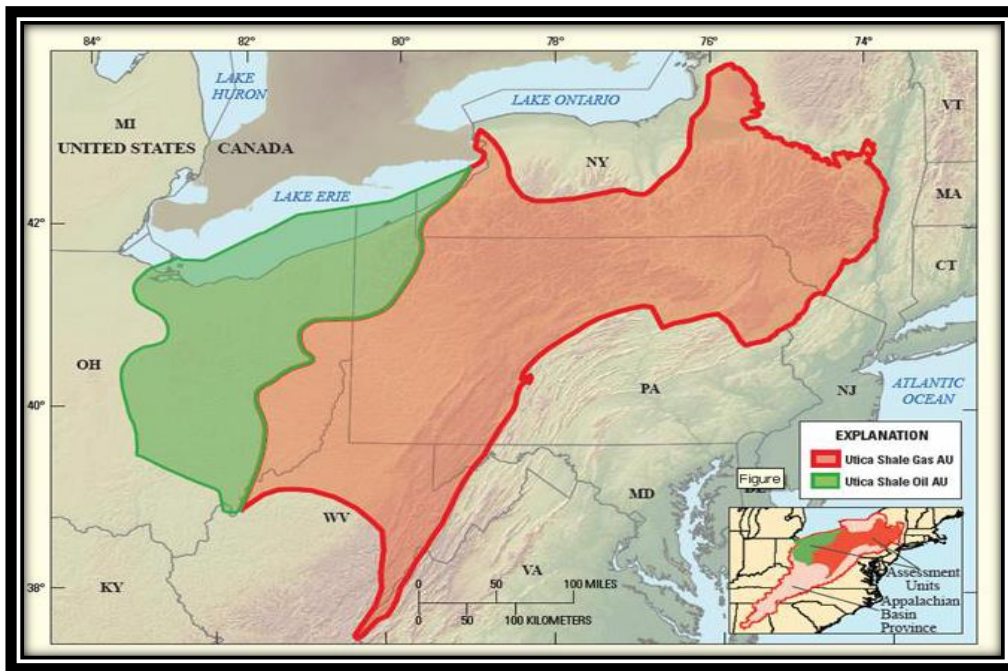
Figure 1-2 Utica Shale oil and gas extent in the Appalachian Basin Province (modified from, USGS, 2012).

The Utica Shale consists of thinly laminated black calcareous shale that is rich in organic matter and was long assumed to be the source of hydrocarbons contained in Cambrian to Devonian reservoirs of the northern Appalachian basin. Deposition of Utica

marine sediments was episodic as evidenced by the alternating limestone and organic-rich shale signaling abrupt deepening of the basin followed by accumulation of more clastic dominated sediments (Paktinat et al., 2007). Total organic carbon (TOC) content across western and southern Pennsylvania, eastern Ohio, northern West Virginia, and south eastern New York ranges from 1% to 3% (Ryder, 2008; Kirschbaum et al., 2012). The Utica shale is characterized by Type II and Type III kerogen (Paktinat et al., 2007; Ryder et al., 2008). Porosity and matrix permeability range for Utica shale is from 3-7 % and 0.08 – 3 μD respectively (Paktinat et al., 2007).

Utica Shale in Ohio – Study Location

In Ohio, the Utica Shale overlies, or in some parts is the laterally equivalent with the Point Pleasant Formation, another organic rich formation. It is believed the latter formation might be more productive than the Utica Shale because of its higher organic content (Harper, 2013; Wickstrom, 2013). However, since the Point Pleasant Formation is principally found only in Ohio, and the Utica is the better-known Formation, the Utica Shale and the Point Pleasant Formation are now mostly referred to as the "Utica Shale" (Thomas, 2012). Exploration and drilling activities in the Utica Shale mostly occur in eastern Ohio (Figure 1-3) where the focus is on oil, condensate, and gas liquids (Riley and Baranoski, 2011). The study area geographically extends from Highlands County in southern Ohio (low hydrocarbon maturity) to Marion County in central Ohio (moderate maturity) and Coshocton County (high maturity) located in eastern Ohio (Figure 1-3).
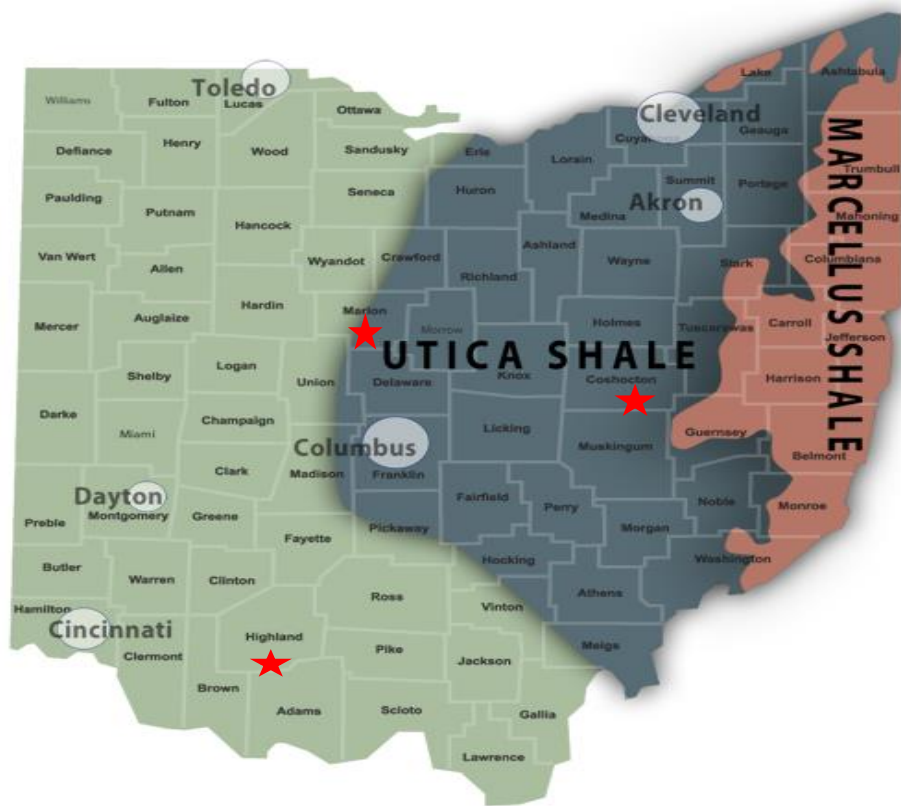
Figure 1-3 Map showing Utica/Marcellus Shale extent in Ohio (modified from – Ohio EPA, 2015) and sample location of cores as red stars

Motivation and Objectives of Study

Tight Oil and natural gas production in Utica Shale has risen by approximately 50% and 60% respectively in the last year. As of February 2015, Ohio Department of Natural Resources (ODNR) estimates that the Utica Shale play had about 1,341 horizontal wells drilled with 729 wells producing hydrocarbon. The reservoirs produce at commercially viable levels with the help of hydraulic fracturing technology which connects a large surface area in the formation to the induced fracture network. However, oil and gas production in such tight shale is still technically challenging, partly from the lack of understanding of nanopore structure characteristics of shale matrix.

Furthermore, despite the improvement in technology, wells in the Utica Shale, like most other shale plays, still experience steep early decline and poor recovery efficiency in production as easily assessed free gas and fluids are produced (King, 2010), with the decline ranging between 55% to 65% after the first year of production (Jarvie, 2010; Figure 1-4). One method to increase productivity is to refracture (refrac) the well, this results in a rebound in production. But, again, always followed by the steep decline curve that is typical to unconventional wells. As a result, oil and gas companies would need to keep drilling more wells to keep output flowing which may not be economical.

Generally, about 95% of hydrocarbon are left behind in the reservoir after primary production, this is because shale reservoirs have extremely tight pores with very low connectivity. Hydrocarbon movement in tight shale is mainly by diffusion with the rate limited by tortuous pathways through sparsely connected nano-sized pores (Ewing et al., 2010; Hu et al., 2012).

Before a shale reservoir is hydraulically stimulated, it is assumed that hydrocarbon molecules fills up the pore matrix at a relatively high pressure. During hydraulic fracturing, the easily assessed free hydrocarbon, through the influence of pressure gradient and diffusion mechanism, move towards the induced fracture network, where (primary) production occurs. However, when the easily assessed hydrocarbons have been recovered, there is a steep decline in production due to drop in pressure in the reservoir and the relatively slow diffusion rate between the hydrocarbons contained in nanopores of the rock matrix and the induced fracture network. Even if a secondary recovery technique is applied, such as refracture "refrac", the above process is repeated again, and a decline in production is still expected.

Fluid and solute transport in rocks are macroscopic consequences of the pore structure, which integrates geometry (e.g., pore size and shape, pre size distribution) and pore topology. Especially when pore connectivity is low, topological factors far outweighs the better known geometrical factors. However, the prevalence of low pore connectivity in some rocks (for example, tight shale), and its impacts on fluid flow and chemical transport are poorly documented and understood (Hu and Ewing, 2014). Understanding the pore structure of these extremely low-connected reservoirs has been challenging task due to limitations of applicable characterization tools and techniques. Recently, the Utica Shale, a huge prospective unconventional reservoir, has been subjected to several studies incorporating different approaches to investigating pore structure characteristics. For example, Swift et al., (2014) characterized Utica Shale at nano- to micro scale using neutron scattering method, Murphy et al., (2013) evaluated porosity and pore system of the Utica Shale using geophysical and geochemical methods. Elgmati et al., (2011) also studied the submicron-pore characterization of shale gas plays, with focus on the Utica, Haynesville and Fayetteville shale gas plays using mercury injection capillary pressure and Scanning Electron Microscope and Focused Ion Beam (FIB-SEM) to determine pore size distribution and characterize submicron-pore structure respectively.

This research work focuses on the pore structure and fluid migration pathways in the Utica Shale using complementary laboratory experiments and network models. It will help bridge the gap between pore topology and fluid flow from tightly connected nanopores in shale rocks and how it affects hydrocarbon recovery from hydraulically stimulated shale formations.
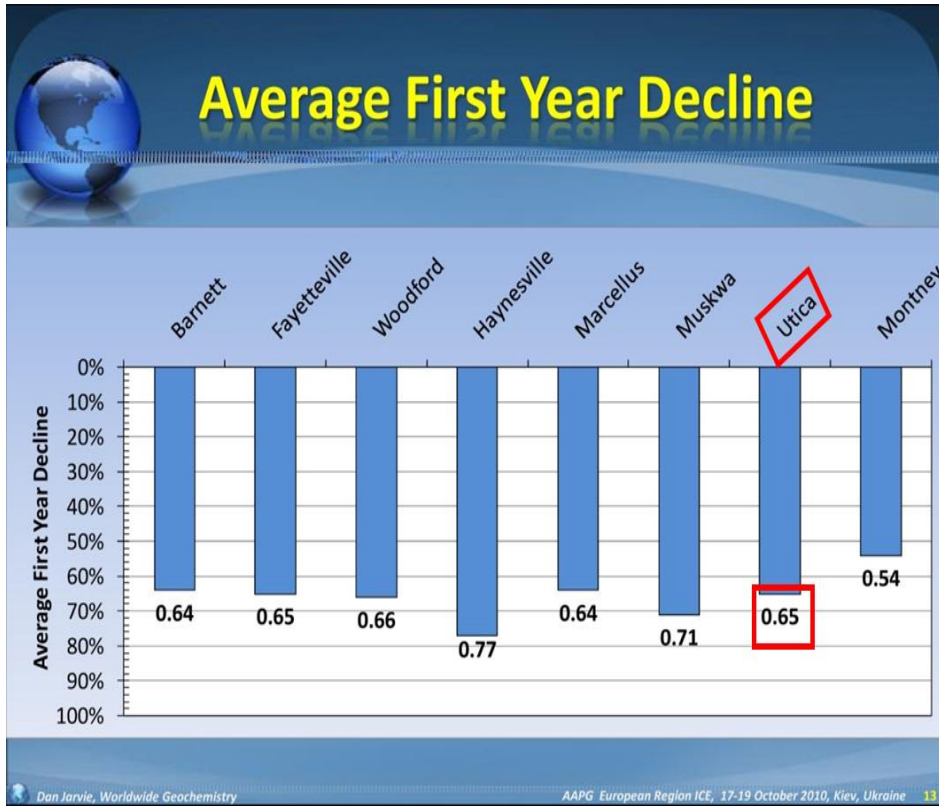
Figure 1-4 Average first year production decline across shale plays (modified from Jarvie, 2010).

Chapter 2

Geologic Setting and petroleum Potential of the Utica Shale

Geologic Setting

The Appalachian Basin is a composite, retroarc foreland basin, containing Paleozoic sedimentary rocks of Early Cambrian through to early Permian age (Ettensohn, 2008). The basin is about 1000 miles long and as much as 350 miles wide, with an area of nearly 230,000 miles (Witt, 1993), extending from southern Quebec in Canada through New York, Pennsylvania, eastern Ohio, West Virginia, western Maryland, eastern Kentucky, eastern Tennessee, northwestern Georgia to northern Alabama (Figure 2-1) in the United States (Ettensohn, 2008). It is bounded to the west by the Cincinnati Findlay and Algonquin arches and on the east by metasedimentary, metavolcanic and intrusive Precambrian and Paleozoic rocks of the Adirondack dome, Blue Ridge and New England Uplands. Updip erosional limit of Paleozoic sedimentary rocks along the Laurentian and the Frontenac arches of the Canadian Shield marks the northern boundary of the basin, and in the southern boundary, it is transitional into the Black Warrior basin (Ettensohn and Brett, 2002). The basin mostly developed on a Late Precambrian-Cambrian, extensional, passive margin generated by the breakout of Laucretia from the supercontinent Rodinia. This formed the adjacent Iapetus Ocean during the Grenville orogeny during 750-535 Ma. Development of the Appalachian foreland basin began with the advent of the Taconian orogeny at 472 Ma and continued for nearly 200 Ma. Sediments were shed to the northwest and accumulated in the foreland basin during this time. This pattern of sediment shedding and accumulation were repeated during the Late Devonian Acadian orogeny and the Late Pennsylvanian. These orogenies are known respectively as the Acadian and the Late Pennsylvanian Alleghenian orogeny.
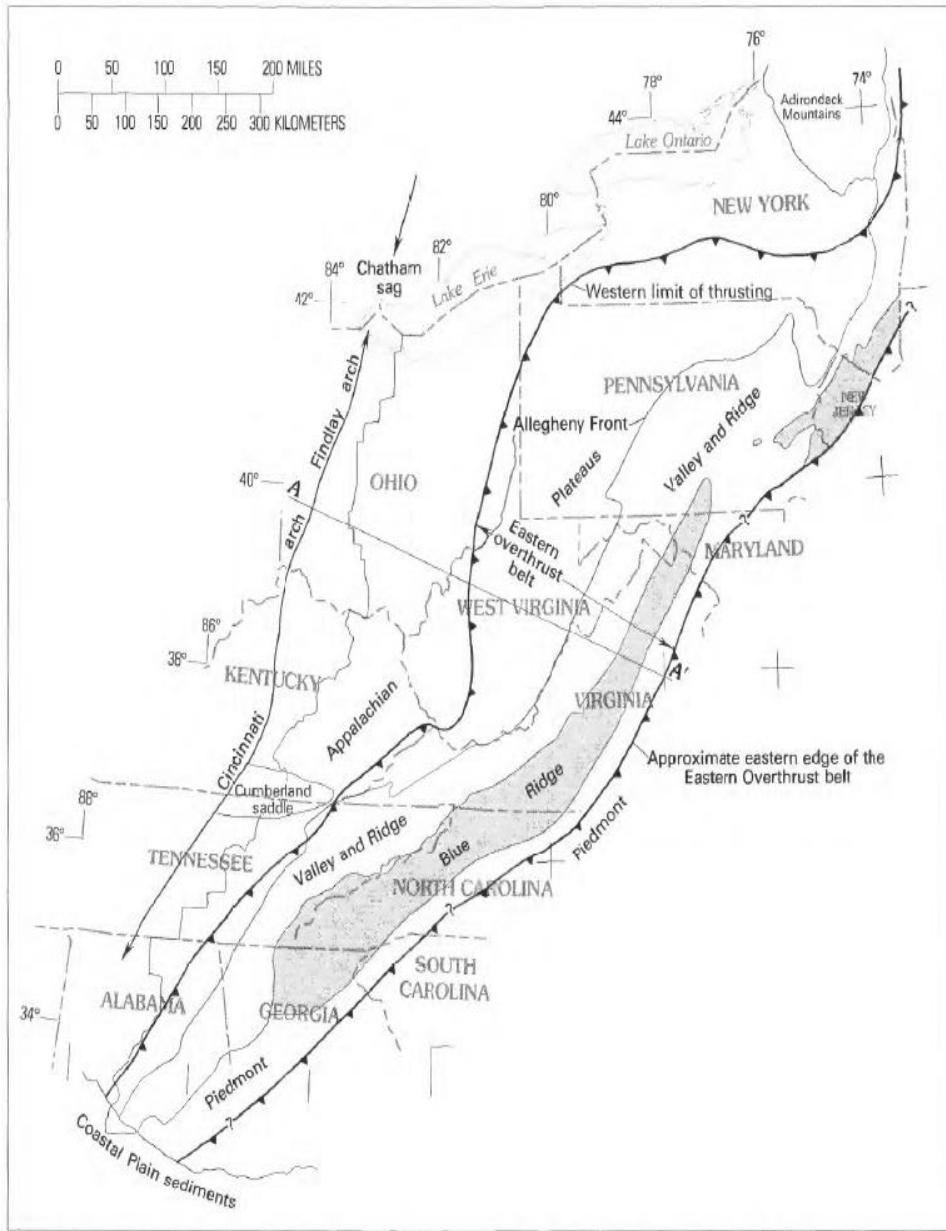
Figure 2-1 Structural map showing the extent of the Appalachian basin (modified from Watts, 1998).

Stratigraphy of the Utica Shale in the Appalachian Basin

In Ohio, a significant unconformity developed along the Cambrian – Ordovician boundary. This was followed in Early Ordovician times, by a eustatic sea level rise leading to the formation of a continental wide passive margin (Cheng, 2014). In Ohio, the passive margin succession is recorded in the Beekmantown Group, which is dominated by intertidal to shallow subtidal limestone limestones and dolostones deposited in responses to high-frequence sea level fluctuation (Salad and Hersi, 2012).The Utica Shale overlies the Lexington Limestone and underlies the Kope Formation (Figure 2-2). The Utica Shale consists of dark-grey platy, finely laminated, calcareous, organic-rich shale with interbedded limestone (Patchen et al., 2006). Upper Ordovician rocks form the Cincinnatian Series. They are consists of about 750 feet of interbedded limestones and shales and contain a diverse array of preserved fossils. The Cincinnati Series have been divided into a number of formation (Figure 2-2). Overall, the Cincinnatian rocks represents a transgressive sequence in which most shale-dominated units represents deposition in deeper, quieter waters and the limestone-dominated units represents deposition in clearer, shallower waters (Hansen, 1997; Patchen et al., 2006).

Structural Framework of the Utica Shale in the Appalachian Basin

Figure 2-3 shows the geologic structure on top of the Trenton Limestone in the Appalachian basin. Because the Utica Shale sits directly on the Trenton Limestone throughout the region, the map equates to a structure map on the base of the Utica
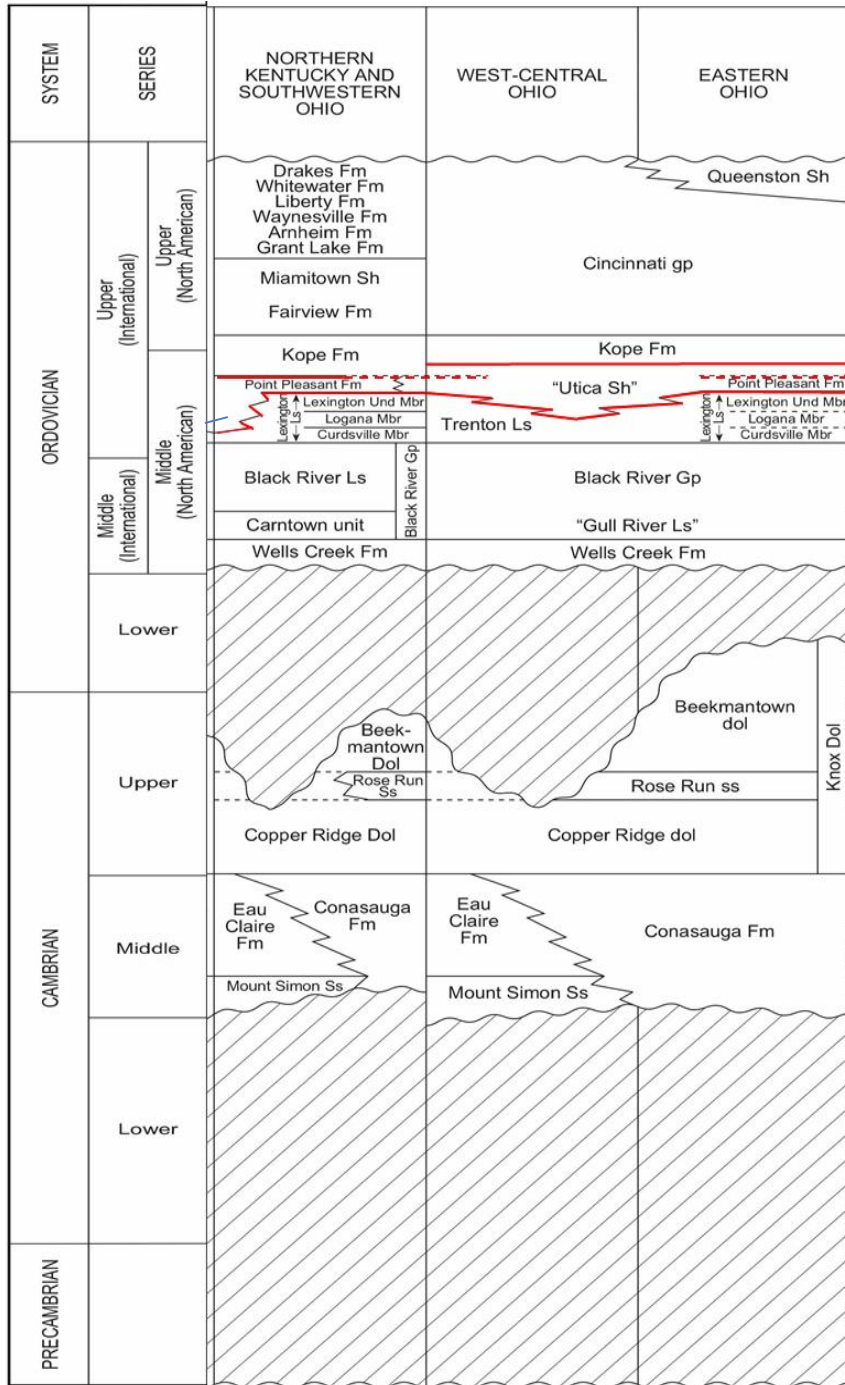
Figure 2-2 Stratigraphic column of Ohio. Utica/ Point Pleasant Formation is highlighted in red modified from Patchen et al., (2006).

facies. Deposition of Trenton platform carbonates and contemporaneous interplatform shales brought about major sedimentological and structural changes to the region as a direct result of the ensuing Taconic Orogeny. As the orogenic activity increased and the foreland basin deepened, the organic-rich Utica Shale transgressed the area overwhelming and drowning carbonate environments (Wickstrom, 2013).

The Taconic orgeny was a complex series of orogenic episodes spread over large part of the Ordovician, it consists of three episodes the first of which occurred during the Early Ordovician in northern New England, The second episode during the Middle Ordovician and the third episode occurred during the Late Ordovician with the largest amount of disturbance in the central Appalachian (Harper, 2013). Flexure of the Laurentia during the orogeny created some deep sedimentary basins that accumulated as much as 1000 feet of sediments in some areas.

Disconformites interrupted what otherwise would have been continuous carbonate accumulation, and widespread deformation occurred. The Utica Shale which is bounded by disconformities, implies that each resulted when a pulse of tectonic subsidence occurred in the foreland basin, followed by a pulse of siliciclastic sedimentation (Harper, 2013). A shift in the basin axis throughout the late Middle Ordovician and early Late Ordovician. The basin axis migrated about 60 miles westward, resulting from deformational loading of the continental margin and progressive foreland flexure, with smaller-scale structural elements, and normal fault-bounded basemen blocks superimposed on large-scale geometry of the Taconic-foreland basin (Harper, 2013).

Petroleum Potential of the Utica Shale

The "Utica Shale" was first used by Emmons (1842) to refer to the black shale in the Mohawk Valley, New York. It is a Late Ordovician calcareous shale facies that

represents a major transgression across much of eastern North America (Patchen et al., 2006; Butterfield, 2011). The Utica shale has been described as a massive, fossiliferous, organic rich, thermally mature, black to grey-black shale (Hill et al., 2002). The facies relationship between the Trenton/Lexington and the overlying Utica/Point Pleasant units are the most complex across the region. Locally, the Utica and Point Pleasant display an intertonguing relationship.
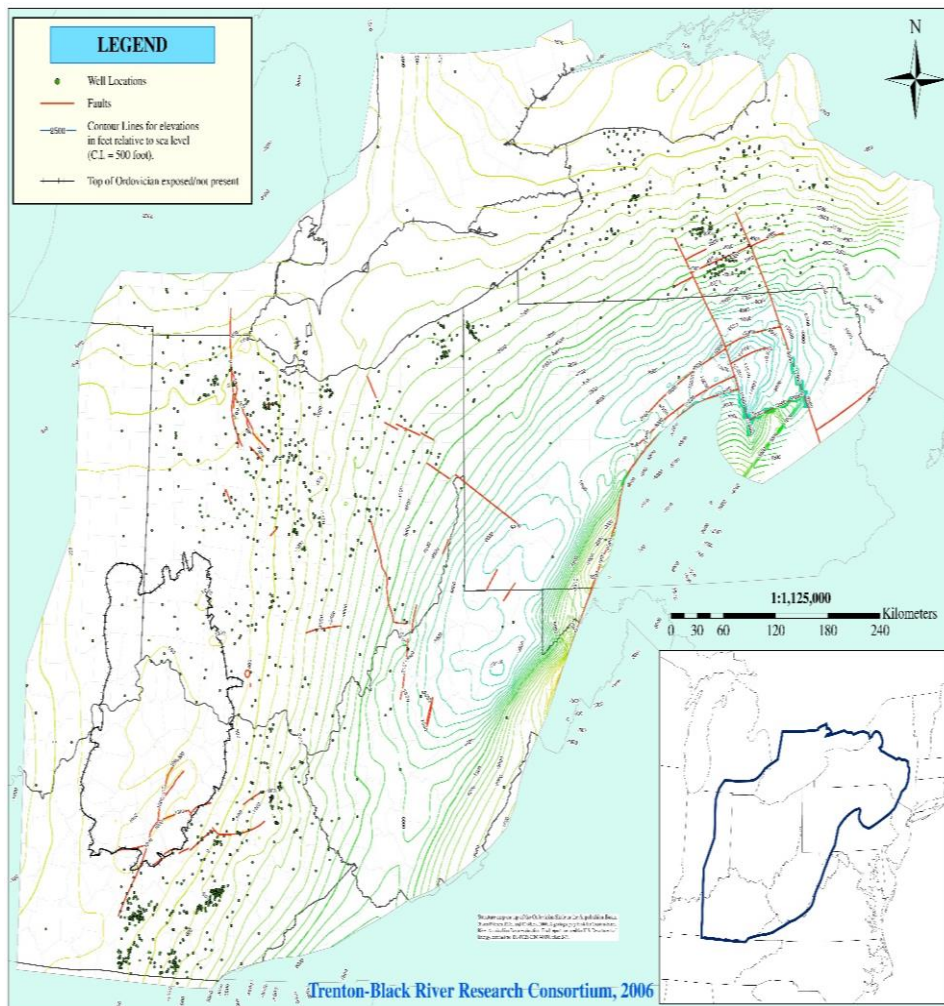
Figure 2-3 Structure map on top of the Utica Shale in the Appalachian basin (modified from Patchen et al., 2006).

The Trenton/Lexington Limestone grades laterally and upward to the dominantly dark-gray to brown-to-black, platy, finely laminated, locally calcareous Utica Shale and interbedded limestone and calcareous shale of the Point Pleasant Formation (Patchen et al., 2006; Harper, 2013). The top of the Point Pleasant is placed at the occurrence of thin, interbedded limestone in the shale interval overlying the Trenton.

The thickness of the Utica Shale is variable, throughout most of its extent, it ranges in thickness from less than 100 feet to over 500 feet (Figure 2-4). Typical thickness for the Utica Shale range from 180 to 230 feet in eastern Ohio, from 175 feet to 250 feet in northern West Virginia, from 320 feet to 350 feet in central Pennsylvania (known here as the Antes Shale), from 150 fee to 250 feet in western New York, and from 350 feet to 700 feet in southeastern New York. (Ryder, 2008).
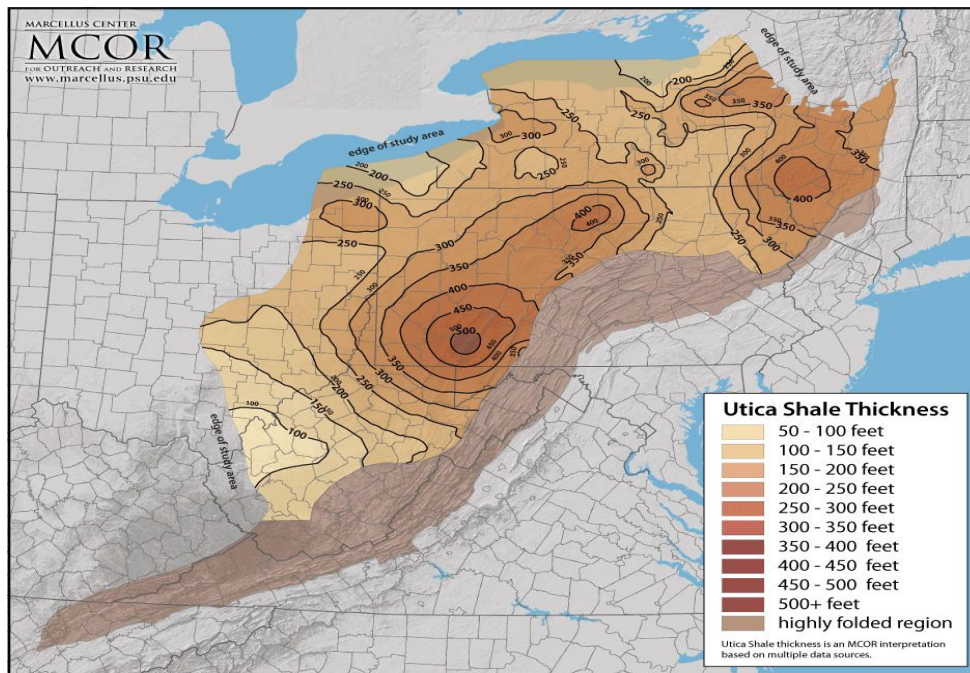
Figure 2-4 Thickness map of the Utica Shale in the Appalachian basin (modified from OHDNR website, accessed 2015).

Mineralogy

The Utica Shale samples collected falls roughly into two mineralogical classes: clay-rich and calcite-rich. X-ray diffraction analysis was carried out on Utica Shale samples from the Fred Barth #3 and Prudential (1-A) wells in eastern Ohio by Weatherford Laboratories (2009). Figure 2-5 shows the average mineralogy of Utica Shale from these two wells which are within the study region. The Utica Shale samples are rich in calcite (~41%), illite (~22%) and quartz (~15%), with low amount of feldspars, plagioclase and kaolinite.
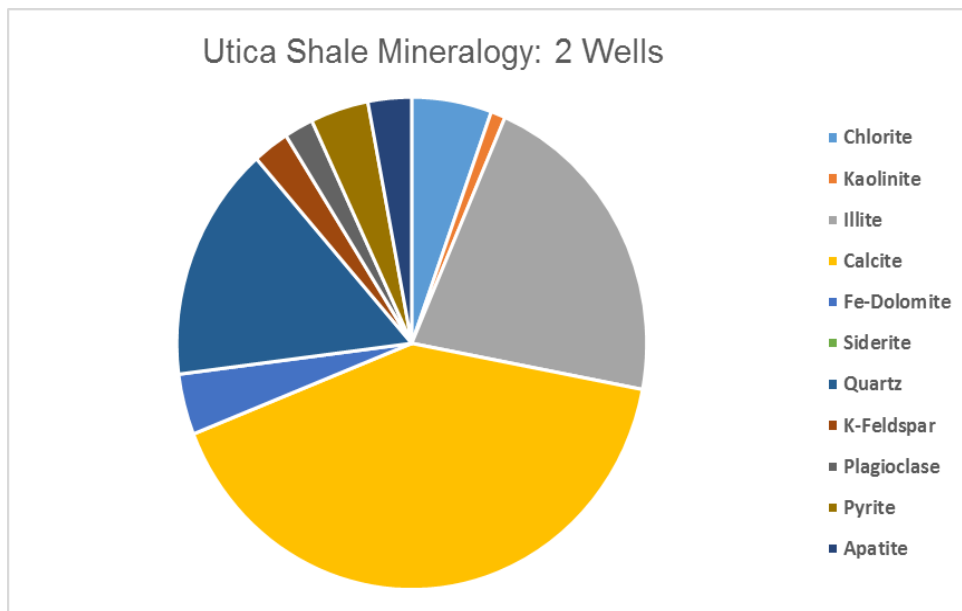
Figure 2-5 Utica Shale mineralogy from Fred Barth and Prudential wells within the study area.

Burial History and Thermal Maturity (%R_o)

The Utica Shale has been considered as an excellent source rock for conventional hydrocarbon exploration in Ohio (Ryder, 1992; Ryder, 2008; Kirchbaum et al., 2012; Wickstrom, 2013). Burial and Thermal history analysis conducted by Rowan (2006)

indicated that the Utica Shale in eastern Ohio and parts of West Virginia entered the oil-window between Late Devonian and Late Pennsylvanian time, and the Utica Shale entered the gas-generation window between Middle and Early Permian time.

Several thermal maturation indicators (T_{max}, vitrinite reflectance, transformation ratio, or production index) indicate that the Utica Shale is a mature succession with an eastern maturation increase from oil window to condensate zone to dry gas zone in Ohio (Figure 2-6). Samples for this study were collected from three wells with varying degree of maturation. Vitrinite reflectance indicator (R_o) is the most commonly measured and widely quoted thermal maturity parameter in the oil and gas industry. It also serves as a de facto reference scale for thermal maturity of organic matter. R_o value range of $0.6 \leq \%Ro \leq 1.4$ is referred to as the "oil window" or thermal maturity range of significant oil generation in oil-prone source rocks. R_o values of between 1.4 and 3.0 represents the "gas window" or maturity range for thermal generation of hydrocarbon gases (Rowan, 2006). In southern Ohio, immature cores were collected from the J. Goins well ($R_o < 0.5$), in central Ohio, moderately mature cores were obtained from the Prudential well ($R_o \sim 0.5\text{-}0.6$). Matured ($R_o \sim 0.80\text{-}0.83$) cores were collected from the Fred Barth well located in eastern Ohio (Figure 2-6; Table 3-1)
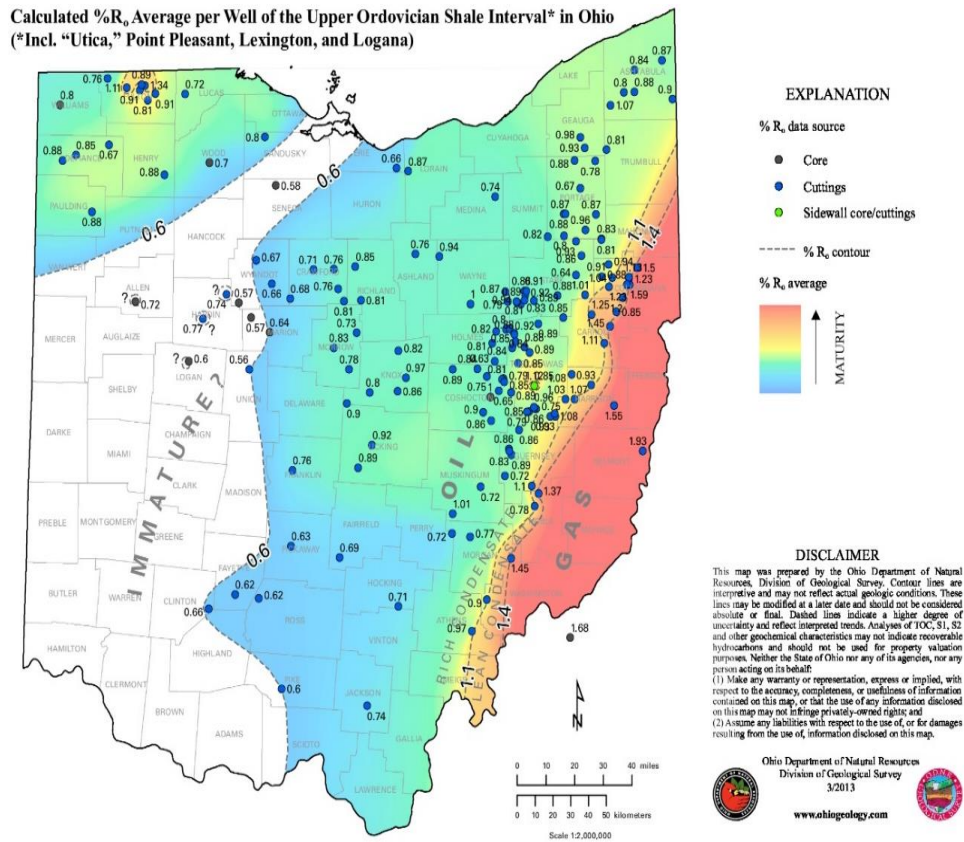
Figure 2-6 Calculated R_o average of Utica Shale in Ohio (modified from Ohio DNR, 2013).

Organic Geochemistry – Total Organic Carbon (TOC)

The Utica Shale is considered to be an oil-prone source rock containing Type II and Type III Kerogen and is recognized as the major source rock for Cambrian through Lower Devonian reservoir rocks. The Shale typically contains 1% TOC, and ranges from 2%-3% TOC in eastern Ohio (Figure 2-7), northern West Virginia and southern Pennsylvania. (Ryder et al., 2012; Hucks, 2013). For samples collected from J. Goins wells, TOC value is about 1.6%, the Prudential well has a TOC range of 2%-3% and the Fred Barth well have TOC value of about 2%-4% (Figure 2-7 and Table 3-1).

19
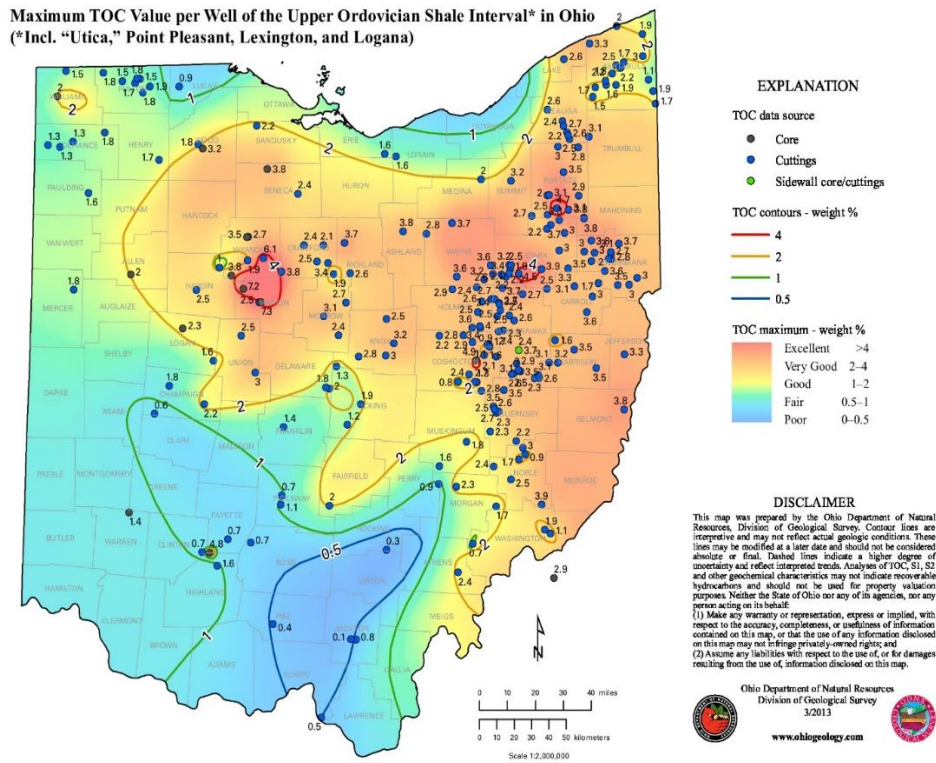
Figure 2-7 Average TOC values of the Utica Shale in Ohio (modified by Ohio DNR, 2013).

Exploration Focus of the Utica Shale

Oil and gas was first discovered in the Utica-Lower Paleozoic TPS in the late 1880's in central Ohio (Ryder, 2008). As at 2002, cumulative production plus remaining reserves in the Utica-Lower Paleozoic TPS represents an estimated 15% to 20% (1.8 to 2.4 billion barrels of oil equivalent BBOE) of discovered oil and gas resources in the basin (Ryder, 2008). Majority of the petroleum discovered to date in the TPS is located on the east-dipping, western flank of the Appalachian basin in central and eastern Ohio, northwestern Pennsylvania, and western New York. Hydrocarbon migration from the Utica Shale to other reservoir formations in the Utica-Lower Paleozoic TPS occurred both vertically and laterally soon after initial oil

20

generation from the Utica Shale from Late Devonian – Late Pennsylvanian time and lasted until the early phases of post-Paleozoic uplift and erosion

As earlier mentioned, the Utica Shale is a vast formation that lies beneath much of northern U.S. despite its vast extent, most of the oil and gas exploration and development activity in the Utica has been focused in eastern Ohio likely for several reasons: 1) the eastern Ohio portion of the play has dry gas, wet gas and is within the oil window, whereas other regions of Utica Shale extent is believed to be dry gas. 2) The Utica Shale in Ohio is boosted by the presence of the Point Pleasant carbonate Formation which enables effective fracture treatment. 3) The Utica is shallower in Ohio, meaning it is relatively less expensive to drill a well with everything else being equal (NGI, accessed 2015). Unconventional hydrocarbon exploration began in the Utica Shale began in 2006 and the first horizontal well was drilled by Range Resources in 2010 in Beaver County, Pennsylvania followed closely by wells in Ohio by Chesapeake Energy in early 2011 (Wickstrom and Shumway, 2014). By the end of 2011, over 150 horizontal permits had been issued and 30 wells drilled. As of February, 2015, Ohio has issued 1799 drilling permits for Utica Shale wells, of those, 1348 wells have been drilled and 740 wells are online and producing.

Chapter 3

Methods

Core Description

Experimental work to characterize pore- structure in the Utica Shale was carried out on samples from different locations with variable porosity, permeability, and thermal maturity values. The differences in petrophysical properties of these samples allowed for investigating the pore structure variation across sample location. Core samples from the Utica Shale in Ohio were obtained from the Horace R. Collins Core Lab Facility through the Ohio Geological Survey Agency located in Columbus, Ohio. Data collection consisted of cores from three wells in Ohio: J. Goins GS-3 (Core API number 34071600090000) located in Concord Township in Highland County (Figure 3-1), Prudential 1-A (Core API number 34101201960000) located in Big Island Township in Marion County (Figure 3-2), and the Fred Barth #3 (Core API number 34031228380000) located in White Eyes Township in Coshocton County (Figure 3-3). Sample details including sample depth (below ground surface), lithology, porosity, and permeability values are shown in Table 3-1. Overall, core preservation is very good, with only short interval cores missing from the Prudential 1-A and J. Goins #3 cores. However, the Fred Barth cores had a few missing intervals. Cores for this study were selected based on availability, hydrocarbon maturity, and presence of the study formation. J. Goins and Prudential core have low and moderate thermal maturity, respectively, based on data available on the Ohio Department of Natural Resources website (OHDNR, accessed in March of 2015). Fred Barth core is a mature core with the well having produced 4063 BBO of oil and 41895 MCF of gas from 1985 to 2013 (OHDNR, accessed 2015). The Utica Formation in Highland County is located at a depth range of 920 feet to 1037 feet, with a formation thickness of 117 feet. At Marion County, the Utica Shale has a thickness of approximately 286 feet with a sampling depth

22

of 1151 feet to 1436 feet. The Utica Shale in Coshocton County has a thickness of about

119 feet and sampling depth is from 5634 feet to 5739 feet. There is an increase in burial

depth of the Utica Shale from southern to eastern Ohio.

Table 3-1 Sample Information

Well Name, API Number, County Latitude and Longitude	Parameters	Value	Source
J. Goins #GS-3 34071600090000 Highland 39.049771 and -83.617628 (low maturity)	TOC (%)	1.6	OHDNR, 2013
	%R_o	~0.5	OHDNR, 2013
	Depth range (ft)/ Formation	940-1021 (Utica Shale)	
	Lithology	Grey shale with limestone	` OHDNR (1987)
Prudential #1-A 34101201960000 Marion 40.587225 and -83.240786 (Moderate maturity)	Porosity (%)	2-3.5	GeoMark, Source rock analysis(2009)
	Permeability (µD)	1.41	GeoMark, Source rock analysis(2009)
	TOC (%)	2.5-3	OHDNR (2010)
	%R_o	0.5-0.6	GeoMark, Source rock analysis(2009)
	Depth range (ft)/ Formation	1149-1436.5/ (Utica Shale)	
	Lithology	Black shale interbedded with limestone	OHDNR (2013)
Fred Barth #3 3403122838000 Coshocton 40.306266 and -81.779898 (Mature)	Porosity (%)	2-4	Wickstrom et al., (2013)
	Permeability (µD)	0.533	Wickstrom et al., (2013)
	TOC (%)	2.5-4	OHDNR (2010)
	%R_o	0.8-0.9	GeoMark, Source rock analysis(2009)
	Depth range (ft)/ Formation	5647-5746 (Utica Shale)	GeoMark, Source rock analysis(2009)
	Lithology	Black shale interbedded with limestone	OHDNR, (1991)

Figure 3-1 Goins # GS-3 core in Highland County, Ohio: core box (left; photo from Ohio Geological   Survey, Horace R. Collins Core   Lab Facility located in Columbus, Ohio) and core plug (right) before they were cut.

Figure 3-2 Prudential 1-A core in Marion County, Ohio: core box (left; photo from Ohio Geological Survey, Horace R. Collins Core Lab Facility located in Columbus, Ohio) and core plug (right) before they were cut.

Figure 3-3 Fred Barth #3 core in Coshocton County, Ohio: core box (left; photo from Ohio Geological Survey, Horace R. Collins Core Lab Facility located in Columbus, Ohio) and core plug (right) before they were cut.

Mercury Injection Capillary Pressure (MICP)

Pore structure characterization of core samples includes measurement of fundamental pore properties such as porosity, permeability, tortuosity and pore size distribution. Other properties analyzed are bulk density and particle density. These parameters were analyzed using mercury intrusion porosimetry (AutoPore IV 9510) manufactured by Micromeritics Instrument Corporation (Norcross, GA) (Figure 3-4) and is available at the University of Texas at Arlington. Mercury porosimetry characterizes a material's porosity and porosity-related characteristics by applying various levels of pressure to a sample immersed in mercury. The pressure required to intrude mercury into a sample's pore is inversely proportional to the size of the pore-throat (Micromeritics, 2001). Mercury injection capillary pressure (MICP) is applicable to pore-throat size range from 3 nm to 300 μm in diameter. This method can also be used to determine broader pore characteristics, such as total pore surface area, tortuosity, percentage total volume, median or mean pore diameter (Micromeritics, 2001; Hu and Ewing, 2014; Hu et al., 2014).

Mercury porosimetry is based on the capillary law governing liquid penetration into small pores. As a non-wetting fluid to most porous media, mercury will not spontaneously invade pores by capillary action unless an external pressure is applied. The diameter of the pore-throat invaded by mercury is inversely proportional to the applied pressure; the higher the applied pressure, the smaller are the pores invaded by mercury. This is expressed in the equation developed by Washburn (Washburn equation) which assumes all pores are cylindrical.

$$\Delta P = -\left(\frac{2\gamma \cos \theta}{R}\right)$$ .... (3.1)

Where,

ΔP – pressure difference across the curved mercury interface (psia);

γ – Surface tension of mercury (485 dynes/cm);

θ – contact angle between mercury and the porous medium;

and R is the corresponding pore-throat radius. Using γ = 485 dynes/cm and θ = 130°, the above equation becomes

$$\Delta P = -\left(\frac{90.43}{R}\right)$$ .... (3.2)

Where R – equivalent pore-throat radius (µm) (Gao and Hu, 2012; Hu and Ewing, 2014).

During the sample analysis, MICP collects the data of applied pressure and induced intrusion volume at a specific pressure (Gao and Hu, 2012; Hu and Ewing, 2014). Although pores are rarely cylindrical, in reality, this equation provides a practical representation of pore distributions yielding very useful and applicable results for most applications.
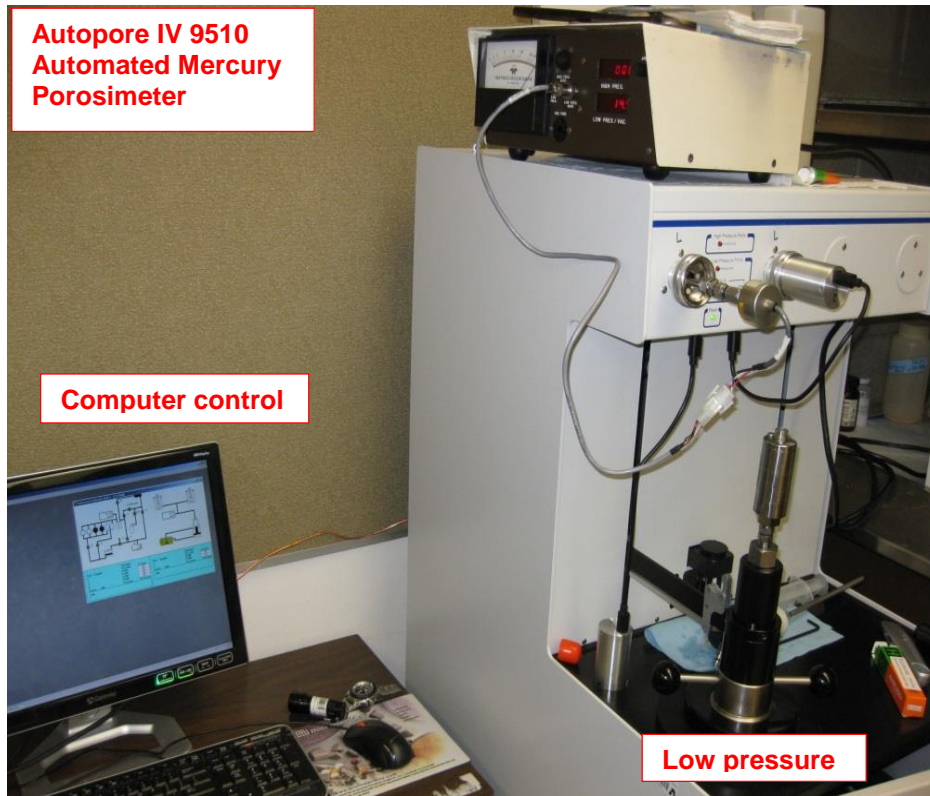
Figure 3-4 Micromeritics Autopore IV 9510

Furthermore, permeability measurement can also be calculated from MICP analyses as highlighted by Gao and Hu, (2012). Permeability measurement for the shale samples were calculated using data of applied pressure and cumulative intrusion volume at a specific pressure derived from MICP measurement. Katz and Thompson (1986; 1987) introduced the following equation to calculate permeability based on MICP data:

$$k = \frac{1}{89}(L_{max})^2 (\frac{L_{max}}{L_c}) \phi \ S(L_{max})$$ .... (3.3)

Where,

K – air permeability (μm)

L_{max} – is the pore throat diameter at which hydraulic conductance is maximum (μm);

27

L_c – is the characteristic length which is the pore-throat diameter (μm) corresponding to the threshold pressure (derived from inflection point on the cumulative intrusion curve) P_t (psia)

Φ – is porosity

$S(L_{max})$ – fraction of connected pore space composed of pore width of size L_{max} (Gao and Hu, 2012).

Procedure for MICP Analyses

Each shale sample (cubes with linear dimensions of about 1 cm) was oven-dried at 60°C for at least 48 hours to remove moisture, then cooled to room temperature (approximately 23°C) in a desiccator with less than 10% relative humidity before the MICP test. To perform an analysis, the sample is loaded into a penetrometer which consists of a sample chamber, connected to a metal-clad, precision-bore and glass capillary stem. The penetrometer is sealed and placed in a low pressure chamber where the sample is evacuated to 50 μm Hg (0.05 torr, 0.000972 psi, or 6.7pa) to remove excess air and moisture. During the MICP test, each sample underwent both low-pressure and high-pressure analyses. Under low-pressure analysis, the mercury fills up the sealed sample cup. A maximum filling pressure of 30 psia and equilibrium time (the minimum time duration to achieve stable mercury level before proceeding to the next pressure) of 10 seconds was set for low-pressure analyses for shale samples. Mercury first fills up pore spaces it can easily access by overcoming the capillary pressure of larger pore-throat with a limit of about 300 μm (depending on the filling pressure used) for low-pressure analysis. For high-pressure analysis, mercury can intrude into pore throats as small as 3 nm at an incremental pressure from 30 psia (end of low-pressure) to 60,000 psia at the equilibrium time of 45 seconds. By measuring the volume of mercury that intrudes into the sample material with each pressure change, and knowing the values of interfacial tension of mercury and

contact angle between mercury and rock sample, values of pore throat radius, porosity, permeability and tortuosity are obtained (Gao and Hu, 2012; Hu and Ewing., 2014). One caution to note when using the MICP approach in determining pore-size distribution is the ink-bottle phenomenon, which is when large pores are connected by smaller neck entrances from the sample surface, and pore accessibility issues causes it to underestimate the volume of large pores and overestimate that of small pores. MICP results are also affected by sample size, and this provides us with an opportunity for examining the pore accessibility of different sized samples (Hu and Ewing, 2014).

Fluid Imbibition and Tracer Migration

Imbibition has been described as the intake of a wetting phase into pore spaces of a porous media by capillary forces (Buckley, 2001; Abe, 2005; Hu et al., 2014). Two types of imbibition processes are common: (1) forced imbibition, where an external force is applied to promote displacement of fluid, and (2) spontaneous imbibition, which is defined as the process when fluid penetrates the capillary media due solely to the potential generated by wettability difference at the solid wall with respect to the contacting fluid (Lopez and Soria, 2007). Spontaneous imbibition is a capillary dominated process and the imbibition rate depends on properties of the porous media, fluids, and fluid rock interaction. Imbibition of fluid into geologic formation is an important phenomenon, particularly in the context of oil recovery hydrocarbon reservoir or production of natural gas from hydraulically-fractured formation (Xie and Marrow, 2001; Abe, 2005; Olafuyi et al., 2007; Chaudhudri et al., 2010). Numerous studies have been performed on the process of spontaneous imbibition. Ma et al. (1999) correlated spontaneous imbibition to dimensionless time and Olafuyi et al. (2007) demonstrated that reliable experimental data can be produced on small (0.3 cm^3) core plugs.

29

This study focuses on spontaneous imbibition of the Utica Shale samples using three fluids (DI water, API brine and n-decane) to model reservoir condition and to observe how these fluids move through pore spaces and, act as a quick way to probe the pore connectivity of the sample. Imbibition tests involve exposing one face of a rock sample to a particular fluid (DI water, API brine or *n*-decane). Using the network modeling results of Ewing and Horton (2002) which is based on percolation theory (a mathematical theory used to analyze properties and processes in disordered systems), we can estimate pore connectivity, as indicated by the slope of log imbibed liquid mass versus log time. In classical homogeneous materials and if gravitational effects are negligible, the distance l to the wetting front increases with the square root of time: $l \sim t^{0.5}$ (Bruce and Klute, 1956; Philip, 1957). If the accessible porosity is uniform with distance, then the cumulative mass of imbibed water l behaves identically; this gives a slope value of 0.5 in log scale. A slope of ~0.25 indicates that connectivity is barely above the percolation threshold and it is assumed that below this threshold, connected pores do not exist. For this study, the imbibition slope range of 0.25 (or less) or 0.5 roughly classifies a rock's pore connectivity. In some cases, the imbibition slope changes from 0.5 to 0.25. This is because the intermediate 0.5 slope can be from the fluid moving through well-connected edge porosity at the sample bottom, and from the wall wetting effect before it migrates through the tightly connected pores in the sample's interior, which is indicative of a 0.2 slope (Hu et al., 2012; Hu and Ewing 2014). Although percolation theory is used in this study to classify pore connectivity, detail of this theory is beyond the scope of this work; readers wanting more information are directed to Stauffer and Aharony (1994), Sahimi (1995), Ewing and Horton (2002) and Hu et al., (2012).

Procedure for Spontaneous Imbibition-

This section discusses the experimental procedure we used in performing spontaneous imbibition test. Utica shale samples were cut into cubes of about 1 cm. All sides except the top and bottom were coated with quick-cure transparent epoxy to allow 1-dimensional imbibition and avoid evaporation of the imbibing fluid (and vapor transport and capillary condensation) through the side surfaces of the samples. The imbibition setup is shown in Figure 3-5. Samples were oven dried at 60°C for at least 48 hours in order to achieve a constant initial water saturation state, and then placed in desiccator to cool to ambient temperature before being subjected to the imbibition experiment. During the imbibition of DI water or API brine, beakers of water were placed inside the experiment chamber to keep the relative humidity high and constant inside the chamber. The top-side of the epoxied sample was loosely covered with aluminum foil, with a small hole left for air escape, to reduce vapor transport and capillary condensation onto the top face. The bottom-face of the sample was lowered to a depth of about 1mm in a fluid (DI water only, API brine or *n*-decane with tracers) reservoir. The imbibition rate was monitored by automatically recording the sample weight change over time using Shimadzu Analytical Balance AUW220D. The imbibition was carried out in a direction parallel to the bedding plane of the sample.

API brine (8% NaCl and 2% $CaCl_2$) has an affinity for the mineral phase while *n*-decane fluid has affinity for the organic matter phase. API brine fluid contains both non-sorbing (perrhenate; ReO_4) and sorbing (cobalt, cesium, europium, and strontium with different sorption extent) tracers and were prepared using ultrapure (Type 1) water and >99% pure reagents ($CoBr_2$, CsBr, CsI, ReO_4, $EuBr_3 \cdot 6H_2O$, $SrBr_2 \cdot 2H_2O$; Sigma-Aldrich Co., St. Louis, MO). Concentrations used were 400 mg/L $CoBr_2$, 100 mg/L CsI, 100 mg/L $KReO_4$, 200 mg/L $EuBr_3$, and 400 mg/L $SrBr_2$.

Imbibition involving *n*-decane with tracers was carried out to examine tracer's association with the organic matter phase. Tracer size for *n*-decane fluid is in nm range [Organic-iodine (1.393 nm×0.287 nm×0.178 nm) and Trichlorooxobis (triphenylphosphine) rhenium (V) (1.273 nm×0.919 nm×0.785 nm)]. Organic-phase tracer chemicals were >99% pure, containing organic reagents [1-iododecane $CH_3(CH_2)_9I$, and trichlorooxobis (triphenylphosphine) rhenium (V) ($[(C_6H_5)_3P]_2ReOC_{13}$)], with the elements iodine (I) and rhenium (Re) from these chemicals readily detected by Laser Ablation –Inductively Coupled Plasma – Mass Spectrometry (LA-ICP-MS).

Imbibition test run-time for DI water was 22-24 hours and for API brine and n-decane, test run-time was 9-12 hours to prevent the tracers reaching the top of the sample. It was also observed that *n*-decane fluid moved through the sample at a much quicker pace than API brine if the rock sample was oil-wet. After tracer imbibition tests, the shale samples were lifted out of the reservoir and were quickly frozen with liquid nitrogen, kept at -80°C in a freezer before freeze-drying (to keep tracers in-place), and then stored at <10% relative humidity before LA-ICP-MS analyses (Hu et al., 2014).
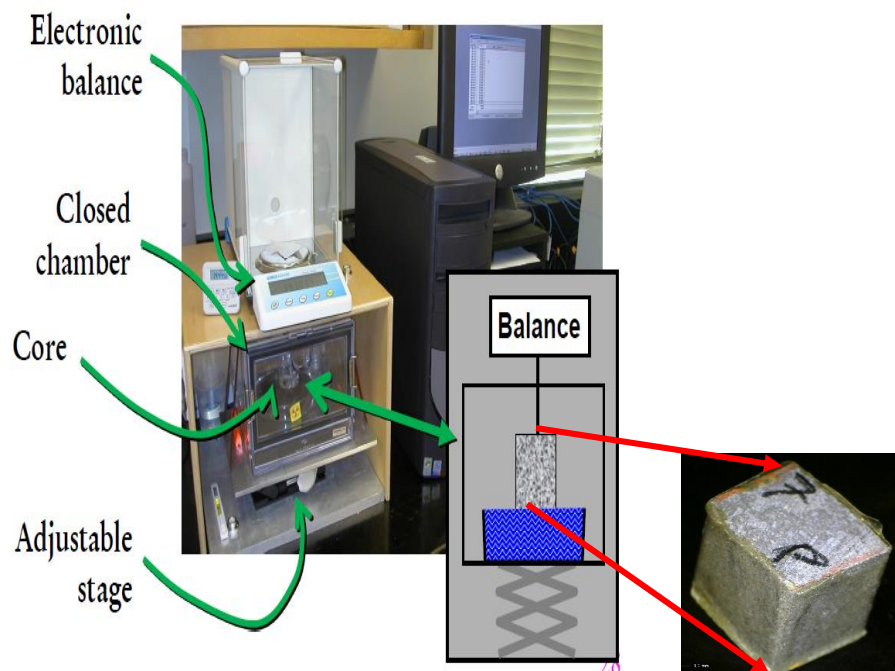
Figure 3-5 Apparatus for imbibition test

Edge-Only Accessible Porosity Test from Vacuum Saturation and High-Pressure Tracer
Intrusion

In rocks with low pore connectivity, accessible pore spaces decrease with a distance from an edge. In this test, we measured the accessible porosity from the edge of the sample (exposed face) using *n*-decane with tracers pumped at low and high pressure in order to fully assess the connected pore spaces in the shale sample. This test aims to observe tracer distribution in connected pore spaces under hydrostatic pressure of 60,000 psia in Utica shale rocks.

Procedure for Edge-Only Accessible Porosity Test from Vacuum Saturation and High-Pressure Tracer Intrusion

This section outlines the process we carried out to determine the edge-only accessible porosity test from vacuum saturation and high-pressure tracer intrusion. The procedure consists of drying samples at a temperature of 60±2°C for at least 48 hours, weighing samples before placing them inside the vacuum chamber (Figure 3-6A) to evacuate air from the edge-accessible pore spaces by flushing with CO_2 several times for at least 24 hours at 0.01 torr (99.999% vacuum). Then the tracer solution (*n*-decane) was introduced as the saturating fluid while the system is still under vacuum. A positive pressure of 60 psia for CO_2 was subjected to the system and the tracers were able to penetrate and occupy the evacuated connected pore spaces. The samples were then quickly placed in a holding compartment made of nitriale glove finger (Figure 3-6B) filled with decane (with tracers), tightly sealed and transferred to the high pressure chamber of MICP apparatus, where an increasing pressure culminating at 60,000 psia was applied to the holding glove fingers; the samples were under the pressure range of 50,000 to 60,000 psia for about 60 minutes. After applying the high pressure, samples were weighed, frozen in liquid nitrogen, kept at -80°C, freeze-dried and then stored at <10% relative humidity prior to LA-ICP-MS analyses.
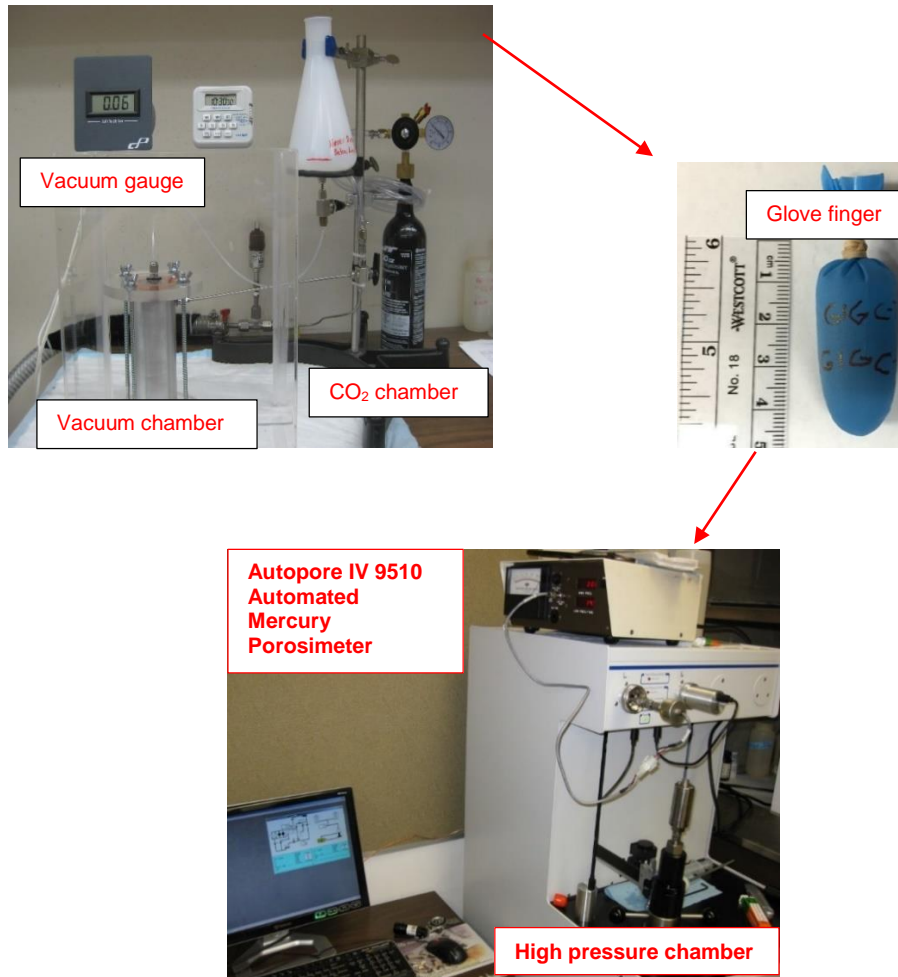
Figure 3-6 Vacuum saturation apparatus (A), tightly sealed nitriale glove finger filled with decane spiked with tracers (B), the glove finger is then transferred to the high pressure port of MICP (C) and a pressure cumulating at 60,000 psia is applied.

Tracer Mapping by Laser Ablation – Inductively Coupled Plasma – Mass Spectrometry

(LA-ICP-MS)

After the tests of tracer imbibition, saturated diffusion and edge-only accessible porosity and high pressure tracer intrusion (in API brine or *n*-decane fluids with tracers), the shale samples were lifted out of the reservoir, frozen with liquid nitrogen, stored at -

80°C in a freezer to keep tracers in-place, freeze-dried at -52°C (to sublimate frozen ice into vapor and leave the tracers in the sample) and then stored at < 10% relative humidity prior to LA-ICP-MS analysis. Laser ablation is the process in which intense bursts of photon energy delivered by short laser pulses are used to vaporize a minute sample mass (in the range of nanogram) sample from a specific sample location. The chemical composition is then analyzed by an (ICP-MS) inductively coupled plasma-mass spectrometer (Hu and Mao. 2012). The laser ablation system (New Wave; Freemont, CA) (Figure 3-7) used a 100 μm spot diameter UP-213 laser to vaporize a hole in the shale sample at sub-micron depth increments; elements entrained in the vapor were analyzed with ICP–MS (PerkinElmer/SCIEX ELAN DRC II; Sheldon, CT). This LA–ICP–MS approach can generate 2-D and 3-D maps of chemical distributions in rock at a spatial resolution of microns, and a concentration limit of low-mg/kg (Hu et al., 2004; Hu and Mao, 2012). An important advantage of the LA-ICP-MS method over other micro-imaging techniques is that little or no sample preparation is necessary prior to analysis, so that chemical smearing accompanying sample preparation is avoided (Hu and Mao, 2012).

Figure 3-7 LA-ICP-MS apparatus for micro-scale elemental mapping

Chapter 4

Results and Discussion

Mercury Injection Capillary Pressure (MICP)

Using MICP measurements, an estimated pore-throat distribution can be determined from the pressure at which mercury was forced into the shale. Figures 4-1A, 4-2A, and 4-3A are plots of cumulative pore volume (%) against the pore-throat diameter of Utica Shale samples at different depths from the J.Goins, Prudential, and Fred Barth Wells, to give an idea of the pore-throat distribution in the study locations. Figures 4-1B, 4-2B and 4-3B shows plots of pore-throat diameter (μm) versus pore volume (%).
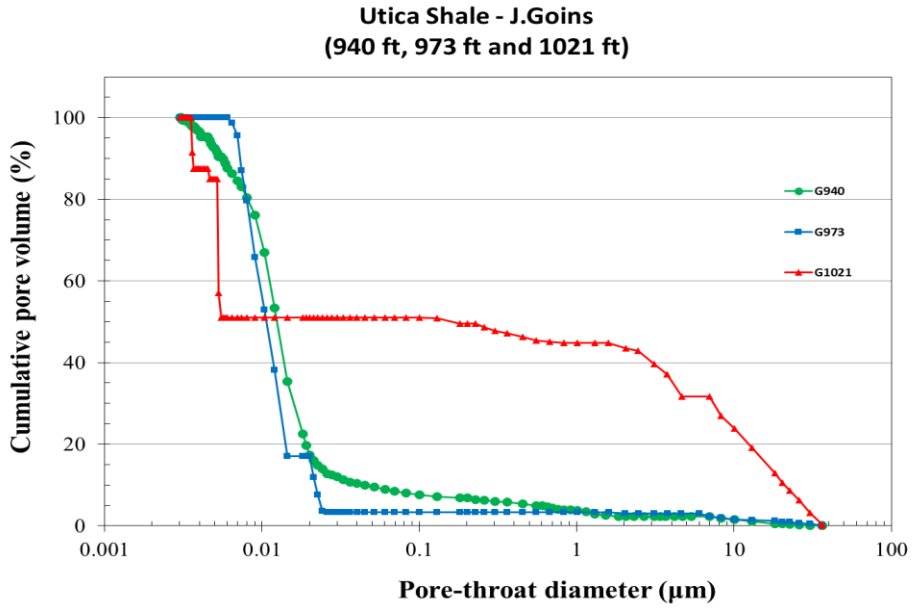
For J. Goins Utica Shale samples with low maturity, 70% - 80% of pore space (by volume) is smaller than 10 μm (Figure 4-1A) and about 70% total porosity (by volume) is found between pore-throat diameter less than 0.01 – 0.05 μm (Figure 4-1B). About 85-90% (by volume) constitutes pore-throat diameter of less than 10 μm (Figure 4-2A) for Utica Shale samples from the Prudential Well, with about 80% (by volume) of total porosity occupied by smaller pores (<0.01 – 0.05 μm; Figure 4-2B). The MICP results for Fred Barth samples (Figure 4-3A) shows that an estimated 60% - 70% pore-throat diameters are smaller than 10 μm with about 50% of total porosity (by volume) being occupied by large pores above (0.1 – 1 μm), and an estimated 42% of total porosity in smaller pore throat range (<0.005 – 0.01 μm; Figure 4-3B).

From the MICP tests, porosity values of ~4.77%, ~1.11% and 0.18% and permeability values of 25.06 nD, 4.99 nD and 0.17 nD were derived for J. Goins Utica Shale samples at 940 feet, 973 feet, and 1021 feet, respectively. For Prudential samples, porosity values are ~5.69%, ~5.50% and 0.45% with permeability values of 5.94 nD, 8.26 nD and 8.71 nD for sampled depth 1149 feet, 1293 feet and 1436 feet, respectively, from the Utica Shale Formation. Fred Barth Utica Shale samples have porosity values of ~0.55%, ~0.38%
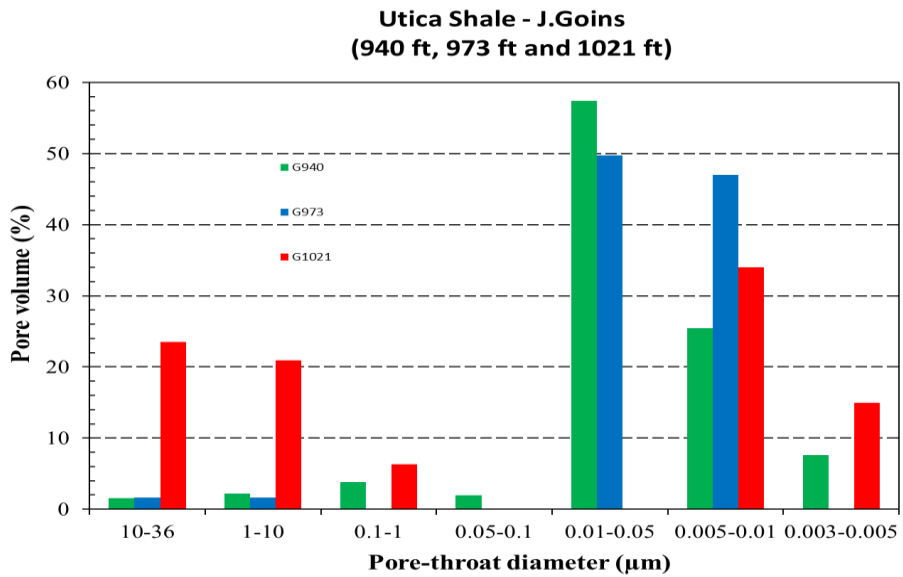
and ~0.38% and permeability values of 0.58 nD, 0.75 nD and 0.63 nD for sampled depth 5647 feet, 5685 feet, and 5746 feet, respectively. Apart from porosity and permeability values, other petrophysical parameters such as bulk density, apparent density and tortuosity values are shown in Table 4-1.

Table 4-1 MICP results for Utica Shale samples

Well name	Sample depth (ft)	Bulk density (g/cm^3)	Apparent density (g/cm^3)	Porosity (%)	Median pore-throat diameter (nm)	Presence of pore-throat less than 3 nm)	Permeability (nD)	Tortuosity
J. Goins #GS-3	940	2.63	2.64	4.770	9.5	No	25.06	5.32
	973	2.63	2.64	1.110	9.2	No	4.99	3.13
	1021	2.59	2.60	0.178	5.3	No	0.17	3.54
Prudential #1-A	1149	2.51	2.66	5.697	4.8	Yes	5.94	11.82
	1293	2.55	2.70	5.502	5.3	Yes	8.26	9.07
	1436	2.56	2.60	0.451	4.8	No	8.71	3.20
Fred Barth #3	5647	2.62	2.75	0.546	4.2	No	0.58	3.81
	5685	2.69	2.72	0.375	5.5	No	0.75	3.04
	5746	2.68	2.69	0.378	4.8	No	0.63	4.76

Utica Shale - J.Goins
(940 ft, 973 ft and 1021 ft)

(A)

Utica Shale - J.Goins
(940 ft, 973 ft and 1021 ft)

(B)

Figure 4-1 MICP measurements showing pore-throat distribution of (A) and Comparison of pore-throat diameter (B) at different depths (940 feet, 973 feet and 1021 feet) for the J. Goins well of Utica Shale.

(A)

(B)

Figure 4-2 MICP measurements showing pore-throat distribution (A) and Comparison of pore-throat diameter (B) at different depths (1149 feet, 1293 feet and 1436 feet) for the Prudential well of Utica Shale samples.

Utica Shale - Fred Barth
(5647 ft,5685 ft and 5746 ft)

(A)

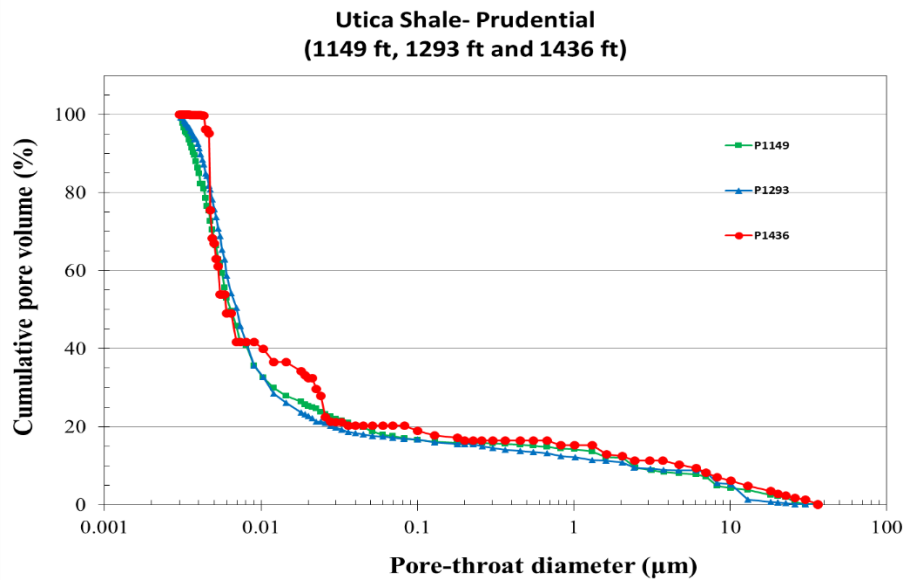
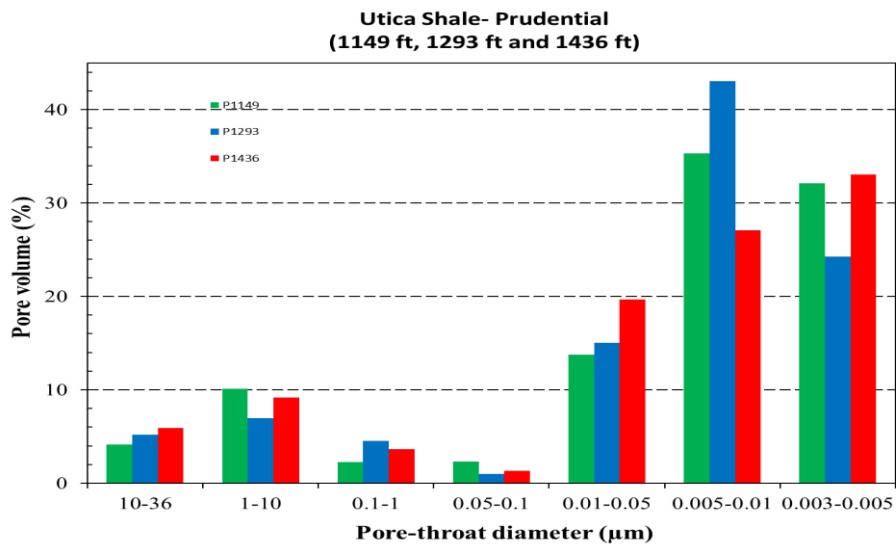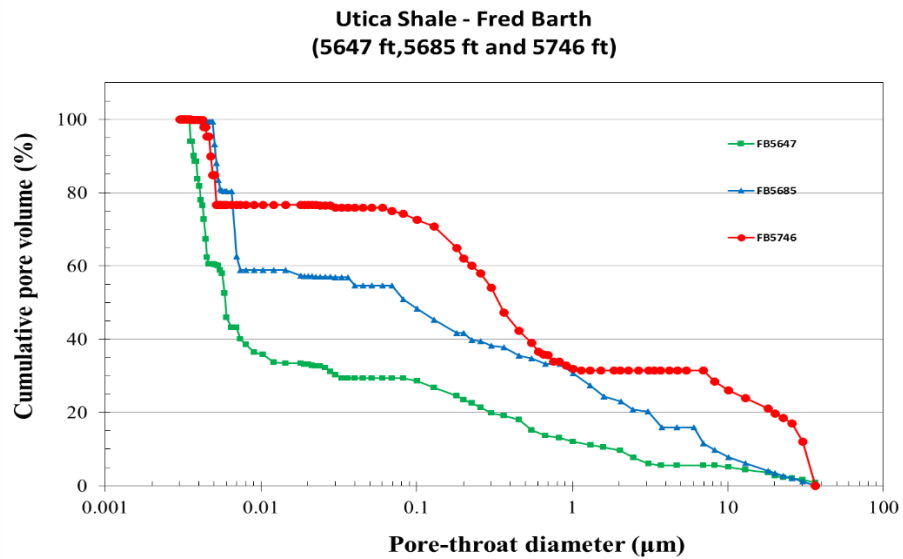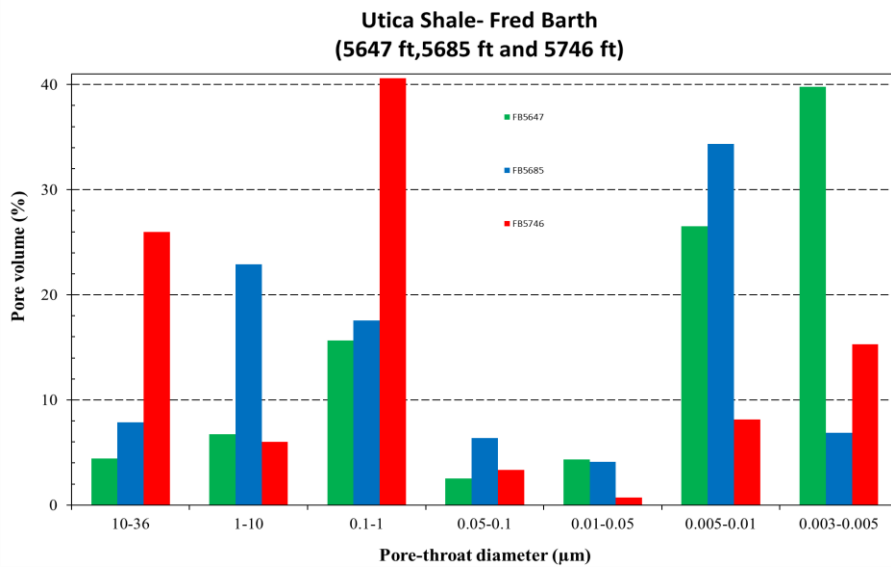**Utica Shale- Fred Barth**
(5647 ft,5685 ft and 5746 ft)

(B)

Figure 4-3 MICP measurements showing pore-throat distribution (A) and Comparison of pore-throat diameter (B) at different depths (5647 feet, 5685 feet and 5746 feet) for the Fred Barth well of Utica Shale samples.

42

It is important to note that at a pressure of 60,000 psia (which is the limit of MICP apparatus), a corresponding pore-throat diameter of ~3.0 nm can be measured. In addition, the cumulative intrusion volume for Figures 4-1, 4-2 and 4-3 is arbitrarily set to 100% for the minimum measureable pore-throat of 3 nm. This suggests that there may be pore-throat diameter less than 3nm that could not be accessed by the MICP apparatus (Table 4-1). Pores less than 3 nm can be quantified by low-pressure gas sorption isotherm approach, however, the volume of inaccessible pore-throat (<3 nm) is not expected to be large enough to play an important role in fluid migration.

Tortuosity is one of the key parameters in describing the geometry and transport properties of porous media (Matyka and Koza, 2012). It can be defined as the ratio of the actual distance traveled between two points to the minimum distance between the two points (Gommes et al., 2009). It characterizes the convoluted pathways of fluid flow through porous rock systems. Tortuosity (L_e/L ratio) values for the Utica Shale are shown in Table 4-1. High tortuosity values (particularly Prudential 1149 and 1293 feet) indicate that fluid particles will need to make way through some convoluted part in order to migrate from one location to another within the Utica Shale. From Table 4-1, the Prudential well has the most tortuous pathways followed by the J. Goins wells with the Fred Barth well having the least tortuous pathway. Based on data collected from MICP, samples show low porosity, very low permeability, high tortuosity, and nm-sized pore-throat range, we believe that the nanopores in the Utica Shale are poorly connected so fluid take longer time to connect pathways of limited distance; this is also shown in tracer imbibition and edge-only accessible test after vacuum saturation and high-pressure intrusion.

Fluid and Tracer Imbibition

Spontaneous Imbibition Results

For spontaneous fluid imbibition (using DI water, API brine and *n*-decane), cumulative imbibition height and imbibition time were plotted in log-log scale for Utica Shale samples from each well at a reference depth (Table 4-2). The steep and noisy initial phase, about 20 – 30 seconds in Figures 4-4, 4-5, and 4-6, is due to the samples settling from the initial contact with imbibing fluid. In some cases (Figure 4-4B, 4-6B-C), a subsequent intermediate-time stable slope of approximately 0.5 is observed. This is apparently caused by fluid migrating up the exterior of the sample as well as the well-connected edge porosity at the sample bottom, which displays classical Fickian behavior. During this intermediate surface migration, imbibition proceeds from all wetted surfaces, the area of which increases with time. After about 30 to 60 minutes, the imbibition slope takes the value of ~0.2 (or 0.3 for *n*-decane fluid), and remains at this value until the sample reaches equilibrium. The predominant 0.2 slope is further evidence that pores in the Utica Shale matrix are poorly connected.

The conducted DI water Imbibition tests produced slopes of 0.224, 0.232 and 0.246 for J. Goins, Prudential and Fred Barth Utica shale samples, respectively (Figure 4-1; Table 4-2), and this result indicates low pore connectivity across the Utica Shale study area. When using *n*-decane as a reservoir fluid, slope values of 0.343 for J Goins well, 0.319 for Prudential well, and 0.343 for Fred Barth well were derived (Figure 4-2, Table 4-2). Using API brine, imbibition slope values of 0.246, 0.191 and 0.189 were derived for J. Goins, Prudential and Fred Barth samples, respectively. Slope values obtained for API brine imbibition are 0.246, 0.191 and 0.189 for J. Goins, Prudential and Fred Barth samples (Figure 4-6; Table 4-2). These slope values are much lower than the slope values observed for *n*-decane. This may be due to the rock sample oil-wet condition as well as its poor pore

connectivity which hinders the movement of API brine fluid through the limited connected pore spaces. It was also observed that *n*-decane fluid was more readily imbibed by the samples at less time than DI water fluid, this may be as a result of the rock samples being oil-wet, meaning that the samples have poor pore connectivity to DI water, but relatively better connectivity to *n*-decane.

Table 4-2 Fluid Imbibition Slopes for Utica Shale

Well Name	Depth (feet)	Hydrocarbon Maturity	Fluid	Sample Dimension (cm)	Imbibition Slope
J. Goins #GS-3	973	Immature	DI water	1.05 L × 1.01 W × 1.09 H	0.224
			API brine	0.96 L × 0.94 W × 1.03 H	0.246
			n-decane	1.05 L × 1.02 W × 0.99 H	0.343
Prudential #1-A	1293	Moderately mature	DI water	1.07 L × 0.99 W × 1.03 H	0.232
			API brine	1.09 L × 1.02 W × 1.00 H	0.191
			n-decane	0.96 L × 0.94 W × 1.03 H	0.319
Fred Barth #3	5685	High maturity	DI water	1.04 L × 1.03 W × 1.05 H	0.246
			API brine	1.08 L × 1.03 W × 0.91 H	0.189
			n-decane	1.07 L × 1.01 W × 1.03 H	0.343
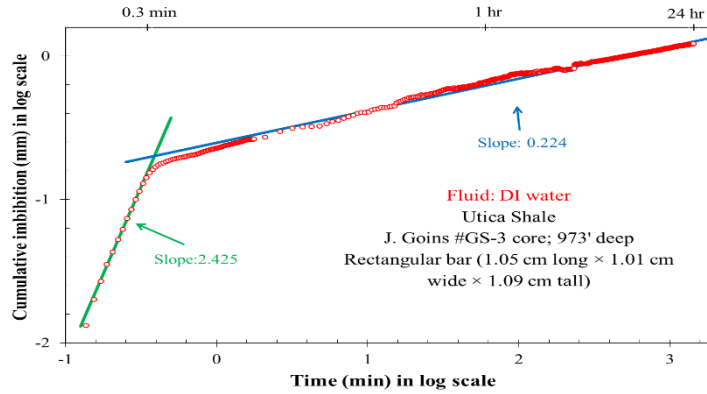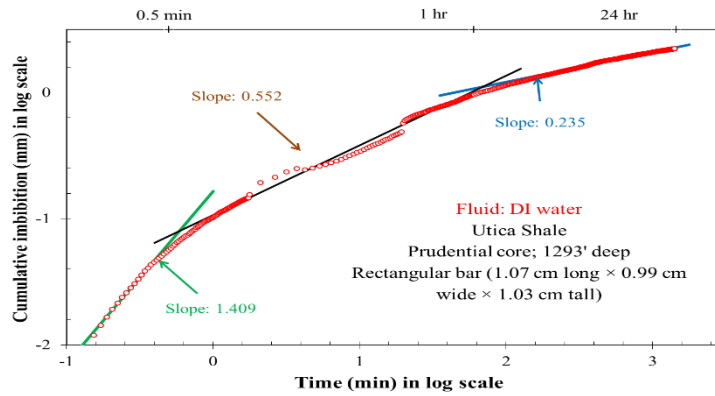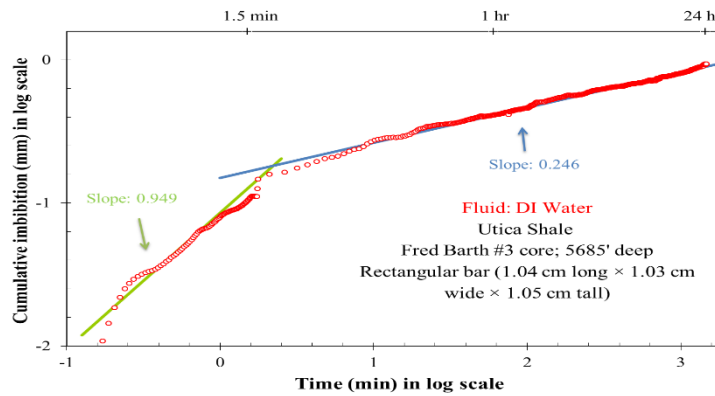
Figure 4-4. Results from DI water imbibition for Utica Shale samples from J. Goins (A), Prudential (B), and Fred Barth (C) Wells showing imbibition curve and slope value.

(A)

(B)

(C)

Figure 4-5 Results from *n*-decane imbibition for Utica Shale samples from J Goins (A),
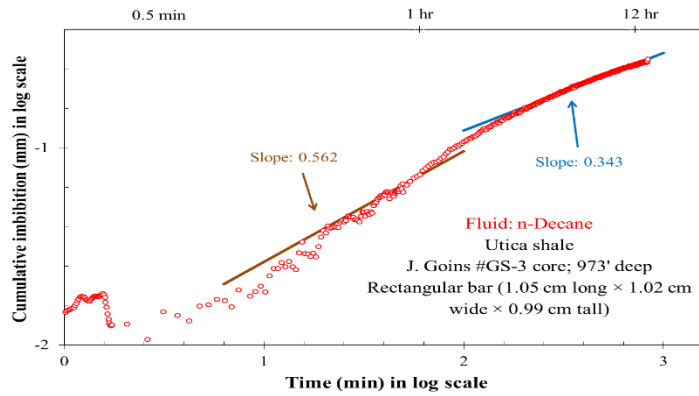Prudential (B), and Fred Barth (C) Wells showing imbibition curve and slope value

(A)

(B)
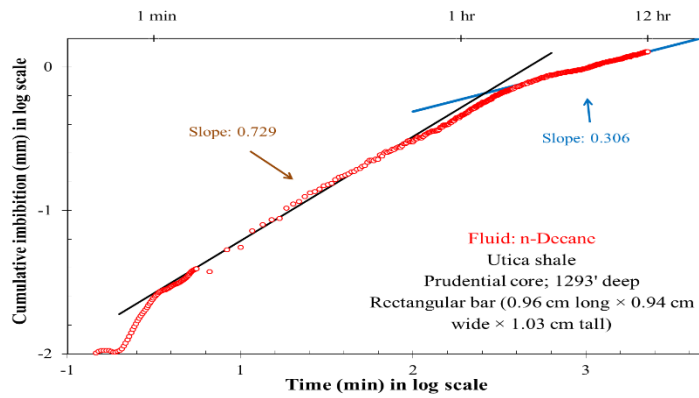

(C)
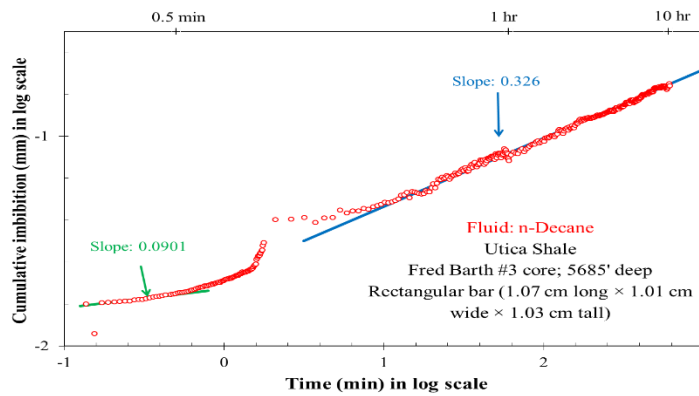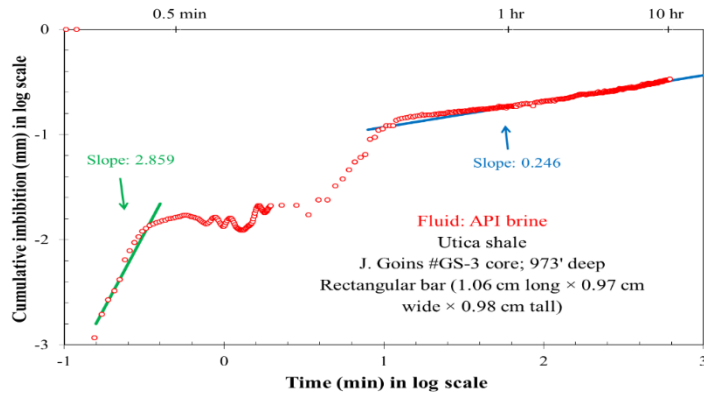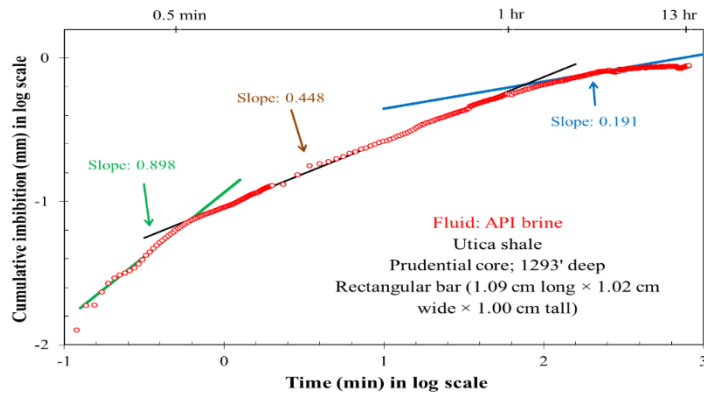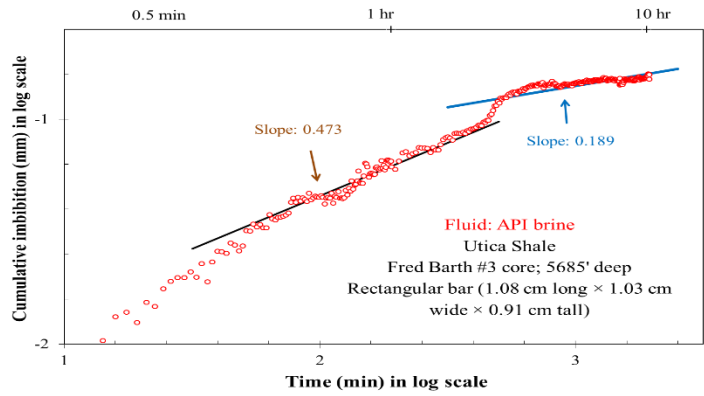
Figure 4-6. Results from API brine imbibition for Utica Shale sample from J Goins (A), Prudential (B), and Fred Barth (C) Wells showing imbibition curve and slope value.

48

n-Decane Tracer Mapping

Results for *n*-decane tracer imbibition into the Utica shale samples are shown in Figures 4-7, 4-8 and 4-9 for J Goins, Prudential, and Fred Barth samples, respectively. After *n*-decane imbibition with tracers, samples were subjected to laser ablation machine, this process vaporizes a hole in the rock sample at micron scale and the vaporized signal is analyzed by ICP-MS. This way, tracer distribution profile, relating to accessible pore space distribution, can be measured. Tracers present in both *n*-decane and API brine fluids are specially designed to examine the kerogen wettability and mineral pore spaces as well as how freely these tracers move through the rocks' accessible pore space.

Figures 4-7, 4-8 and 4-9 shows the bottom, interior and top face mapping for J. Goins, Prudential and Fred Barth samples at reference depths 973 feet, 1293 feet and 5685 feet, respectively, for *n*-decane tracer imbibition. The white portion on the map indicates no tracer penetration in the pore spaces as a result of poor (tiny pore throat) connectivity in the Utica shale rock, the orange and red areas reflects maximum tracer penetration in pore spaces as a results of the tracers ability to access the pore-throat of the sampled region. The light green to blue color distribution indicates minimum tracer intrusion into the pore space of the sampled region. From *n*-decane tracer mapping, observe that iodine tracer (organic-I) penetrated the samples more (Figure 4-7A, 4-8A and 4-9A) than the rhenium tracer (organic-Re; Figure 4-7B, 4-8B and 4-9B) which maybe as a result of the smaller molecular size of iodine tracer (1.393 nm x 0.287 nm x 0.178 nm) compared to the molecular size of rhenium tracer (1.273 nm x 0.919 nm x0.785 nm). Also, notice that high concentration of iodine (organic-I) from the base of the sample through the side and along the top of the sample suggest the tracers being imbibed are "pulled" up by the sample's wall surface (that is in contact with epoxy) and travels faster than tracers moving through the tortuous 3-D pathways within the sample interior. This is referred to as

wall-effect and this phenomenon was observed in the map results of all tracer imbibition samples. Such migration has also been observed and recorded in tracer imbibition and diffusion tests by Hu and Ewing (2014). Through such phenomenon, tracers end up imbibing from both the interior and wall, which gives us an opportunity to evaluate the migration in 3-D and 2-D sample matrix.

LA-ICP-MS analysis for J. Goins sample shows relatively high tracer distribution at the base of the sample for both organic iodine and rhenium tracers, but tracer concentration and distribution deceases as it moves through the tortuous sample interior. Notice an increase in tracer concentration at the top face of the sample, which is probably as a result of tracers migrating through the samples' wall and saturating the top face quicker than tracers moving through the tortuous interior face (Figure 4-7). Overall, J. Goins sample has the least tracer (for both organic-I and organic-Re) penetration and distribution when compared to samples from other two wells. For Prudential sample (Figure 4-8), tracer mapping results show high tracers concentration and distribution from the base of the sample, through the interior, and to the top of the sample for organic iodine tracer. For rhenium tracers (Figure 4-8B), the base of the sample shows high tracer distribution, however, the interior and top faces shows regions of low and no tracer penetration. Organic iodine map result for Fred Barth sample showed very high tracer concentration and distribution at the base and interior of the sample, this reduces slightly at the sample top, with some regions show no tracer penetration (Figure 4-9A). For rhenium tracer mapping, observe the high tracer concentration at the base of the sample and this decreases as the tracers are imbibed through the sample interior to the sample top.
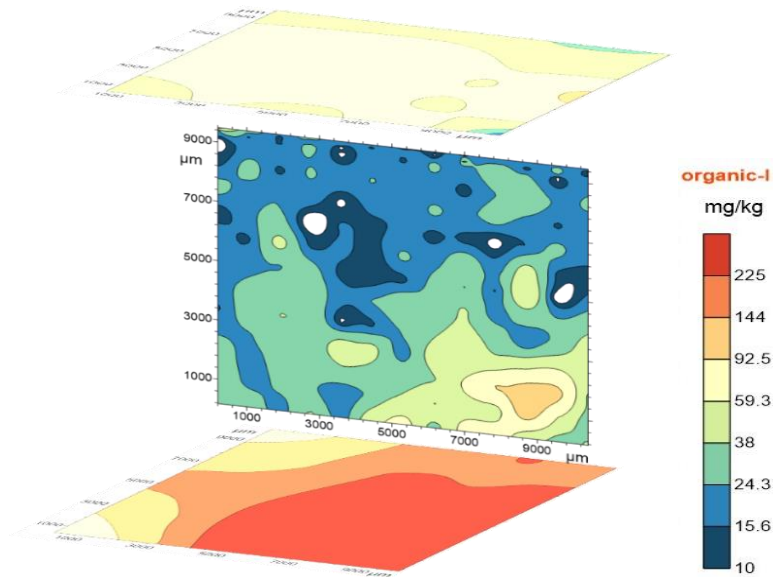
(A)
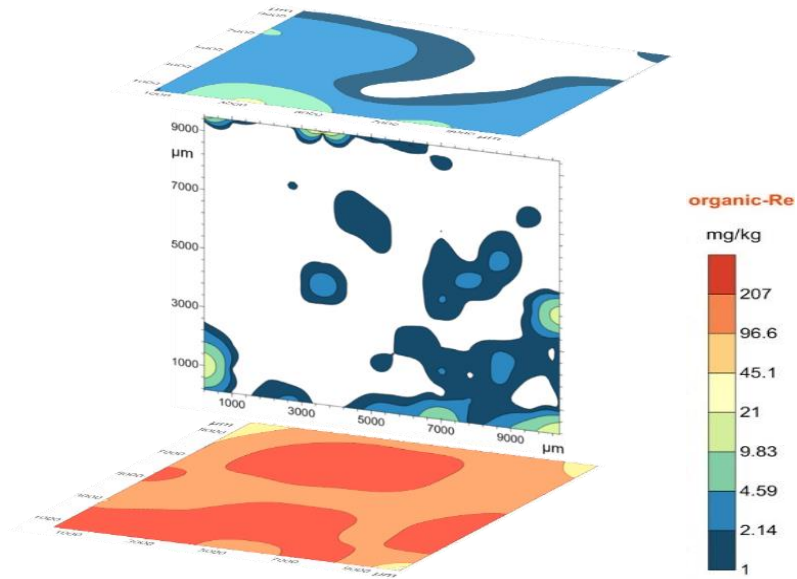
(B)

Figure 4-7. Result from *n*-decane tracer LA-ICP-MS analyses for J. Goins (973 feet). Tracers mapped from bottom (base) face, interior (middle) face and top face of sample using organic iodine tracer (A) and rhenium tracer (B).

(A)

(B)

Figure 4-8. Result from *n*-decane tracer LA-ICP-MS analyses for Prudential (1293 feet). Tracers mapped from bottom (base) face, interior (middle) face and top face of sample using organic iodine tracer (A) and rhenium tracer (B).
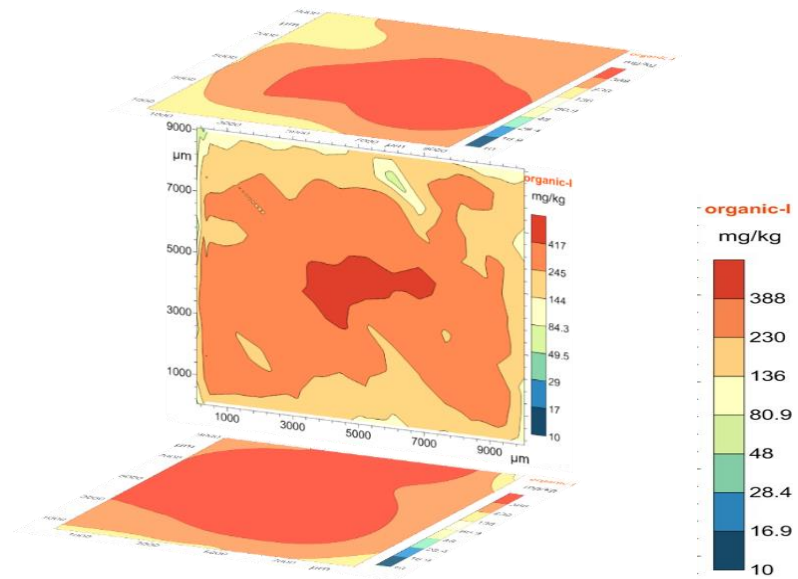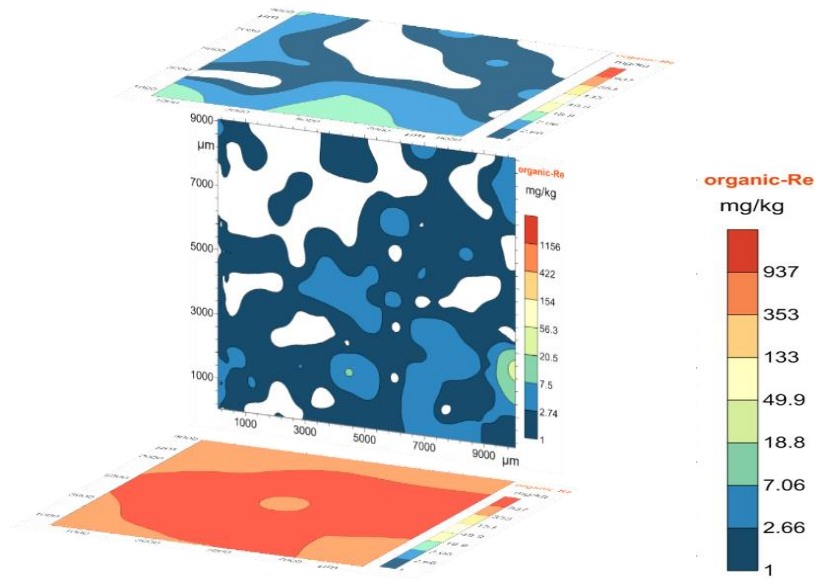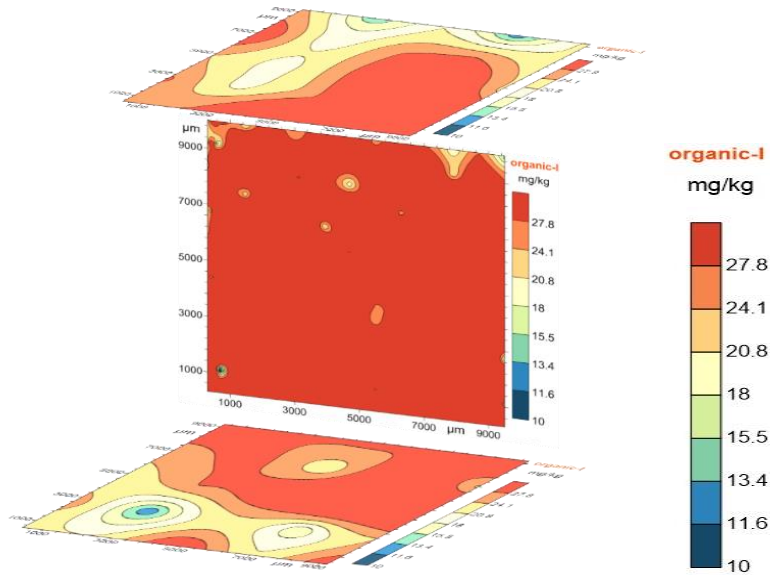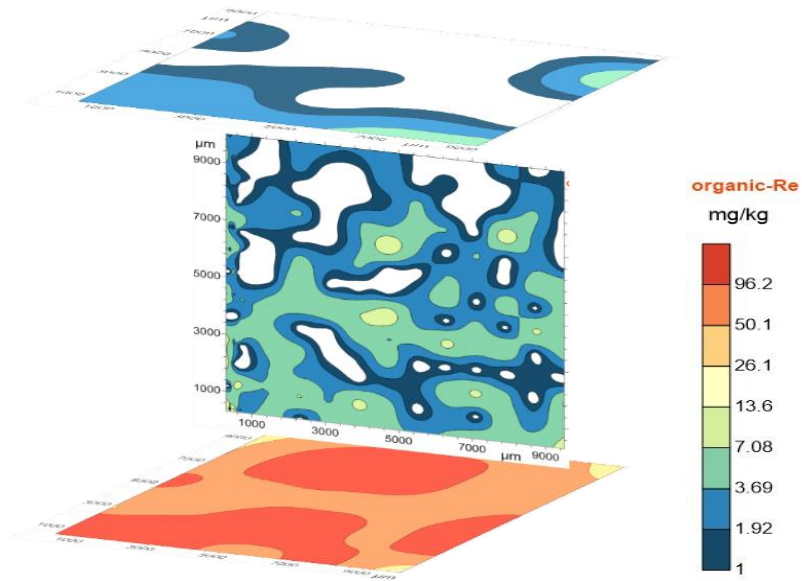
(A)

(B)

Figure 4-9. Result from *n*-decane tracer LA-ICP-MS analyses for Fred Barth (5685 feet). Tracers mapped from bottom (base), interior (middle) face and top face of sample using organic iodine tracer (A) and rhenium tracer (B)
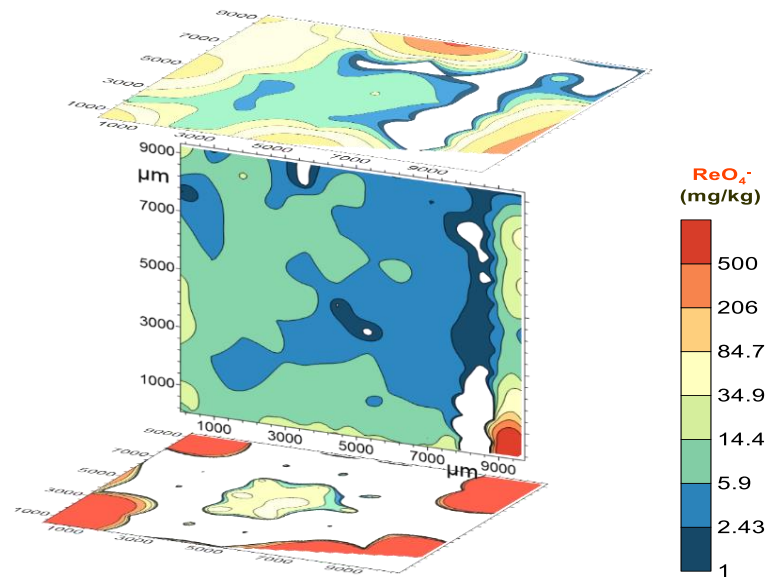
API Brine Tracer Mapping

API brine tracer imbibition samples for Prudential and Fred Barth samples were also subjected through LA-ICP-MS analyses and results from these analyses shows different tracer distribution patterns. The white portion on the map indicates no tracer penetration as a result of very tight pore-throats, the red and orange regions indicate areas of high tracer penetration, and the green to blue regions indicates area of low tracer concentration. The pattern, distribution, and mass concentration of the tracers may also indicate the patterns of pore connectivity within the Utica Shale samples.

Non-sorbing perrhenate (ReO_4^-) tracer will only occupy accessible pore spaces and does not interact with the shale matrix, rather it serves as an indicator of accessible porosity distribution within the sample. Results for API brine tracer mapping for Utica Shale samples from Prudential (1293 feet) and Fred Barth (5685 feet) are shown in Figures 4-10 and 4-11. The tracer map for the base of Prudential sample (Figure 4-10A) shows high ReO_4^- tracer concentration at the sample edge (bottom face) with very low tracer concentration and distribution observed within the sample interior which may be as a result of tracers migrating through the wall of the sample (wall effect). The top face show low tracer concentration centrally, with increased tracer distribution at the wall edges. For europium tracer mapping (Figure 4-10B), the imbibition bottom of Prudential sample indicates high tracer concentration and distribution, the interior and top faces show low tracer concentration centrally, with higher concentration at the wall-edge of the sample indicating wall effect.

Fred Barth perrhenate tracer (ReO_4^-) mapping reveals relatively high tracer concentration and distribution at the imbibition base of the sample, however, there is a virtually no tracer distribution in the interior and top faces (Figure 4-11A) with both faces showing very little concentration. For europium (Eu_3^+) tracer mapping, the base of the

sample indicates high tracer spread, sample interior and top faces shows reduced tracer concentration with some inaccessible pore-throats regions (Figure 4-11B). These results (for both Prudential and Fred Barth samples) show that more europium (Eu^{3+}) tracers migrated through the nanopores of the samples when compared to rhenium (ReO_4^-) tracer. This is probably because of its sorption effect of cationic chemicals of europium tracers onto shale components. Also, note that the bottom face concentration for europium tracers in both Prudential and Fred Barth Utica Shale samples are much larger than rhenium tracers which only occupies pore spaces and does not interact with the shale matrix. The bottom part of the samples are observed to have higher concentrations of tracers which is probably because that part of the sample makes the closest contact with the imbibing fluid as it is submerged in it. Concentration of tracers deceases dramatically with depth illustrating the poorly-connected pore spaces and tortuous pathways of Utica Shale samples.

(A)
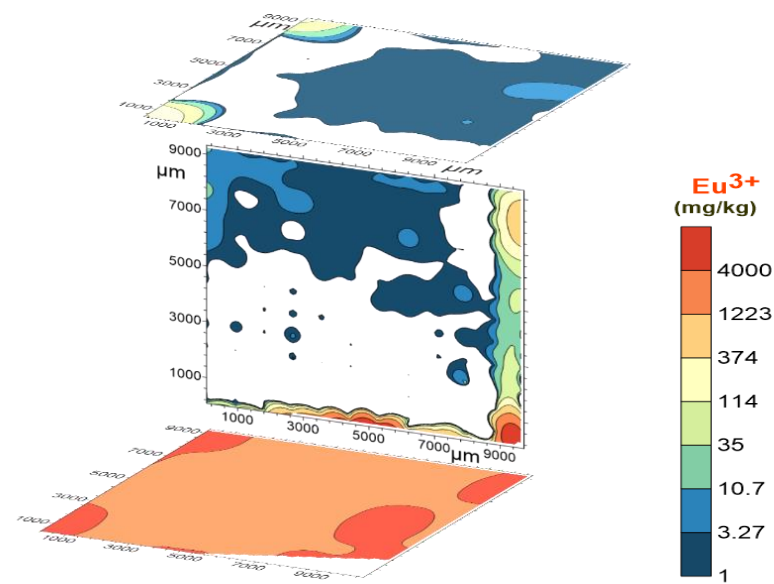
(B)

Figure 4-10. API brine tracer imbibition LA-ICP-MS mapping for Prudential (1293 feet) sample mapped from bottom (base), interior face and top face using API brine using non-sorbing perrhenate (ReO₄⁻) tracer (A) and sorbing Europium (Eu₃⁺) tracer (B).
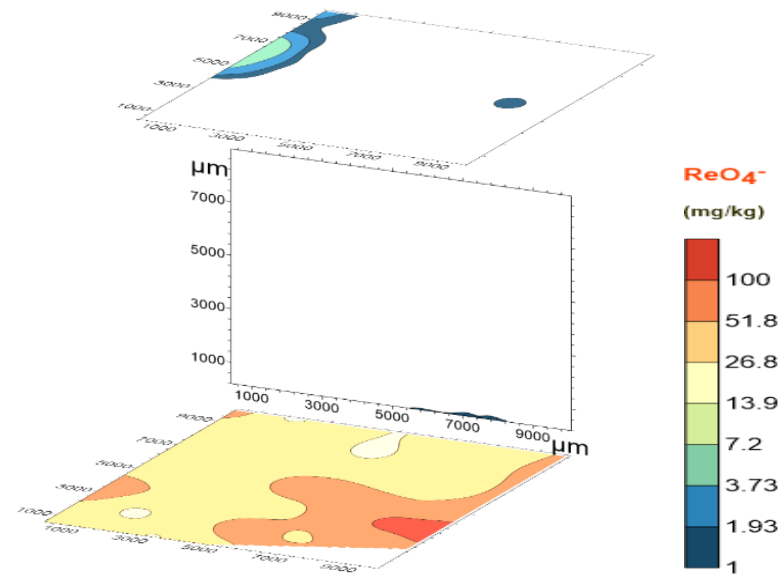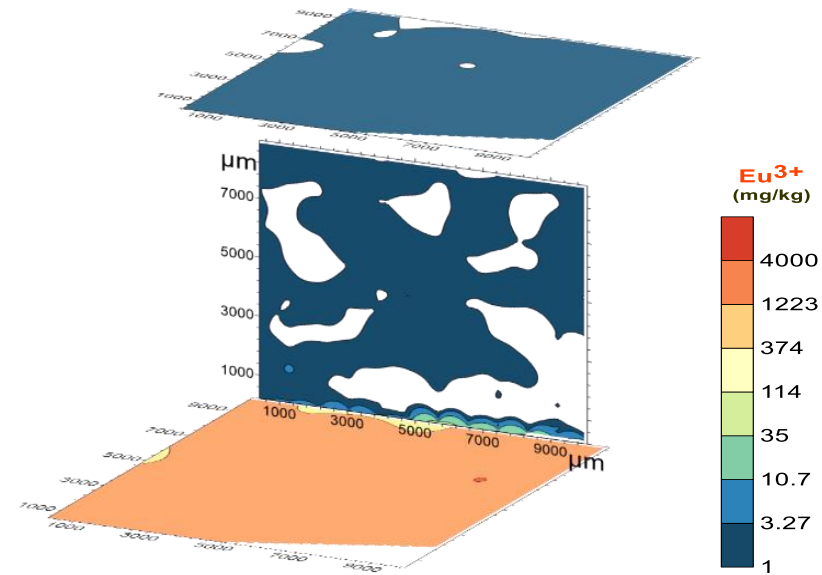
(A)

(B)

Figure 4-11. API brine tracer imbibition LA-ICP-MS mapping for Fred Barth (5685 feet) sample mapped from bottom (base), interior face and top face using API brine using non-sorbing perrhenate (ReO$_4^-$) tracer (A) and sorbing Europium (Eu$_3^+$) tracer (B).

Edge-Only Accessible Porosity Test from Vacuum Saturation and High-Pressure Tracer

Intrusion

Figures 4-12 (Prudential, 1293 feet) and 4-13 (Fred Barth, 5685 feet) shows the mapping results of organic iodine (I) tracers and organic rhenium (Re) tracers, which is indicative of the edge-accessible porosity distribution of the Utica Shale under high pressure of 50,000 psia – 60,000 psia. Organic *n*-decane fluid was used to examine the tracer's association with the kerogen phase. Observe that, though *n*-decane fluid is easily imbibed by Utica Shale samples, there is a dramatic decrease of tracers with depth into the sample (even with the high hydrostatic pressure applied to force tracers into accessible pore spaces) which illustrates the poorly-connected pore spaces of the Utica Shale. It is also observed that the iodine tracer penetrated the samples more than the rhenium tracer (ReO_4^-) which is probably due to the smaller molecular size of the iodine tracers. Generally, tracer concentration reduces with depth into the sample for both Prudential and Fred Barth samples.
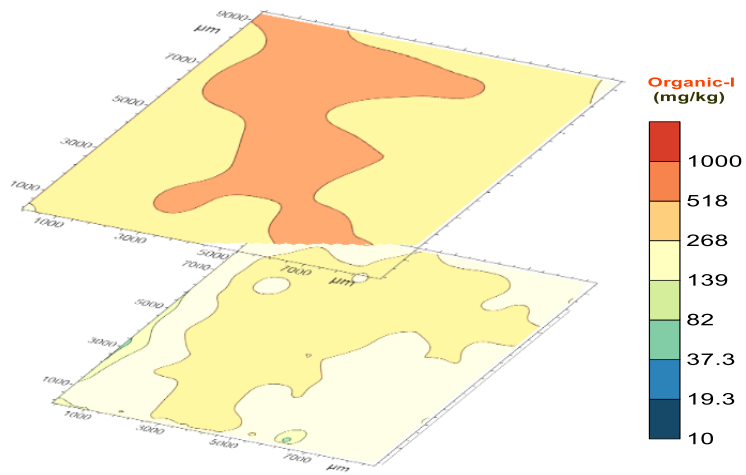
(A)
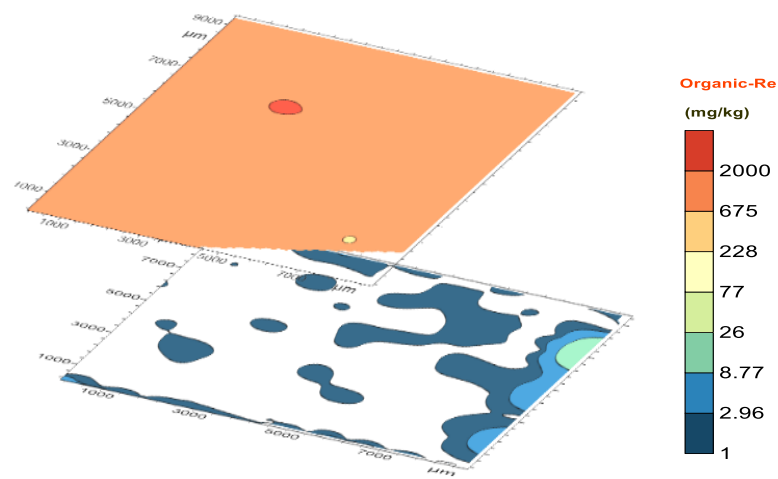
(B)

Figure 4-12. Edge-only accessible LA-ICP-MS mapping result for *n*-decane organic iodine tracer (A) and organic rhenium tracer (B) for Prudential (1293 feet) sample showing top face and interior face.

(A)

(B)

Figure 4-13. Edge-only accessible LA-ICP-MS mapping result for *n*-decane organic iodine tracer (A) and organic rhenium tracer (B) for Fred Barth (5685 feet) sample showing top face and interior face.
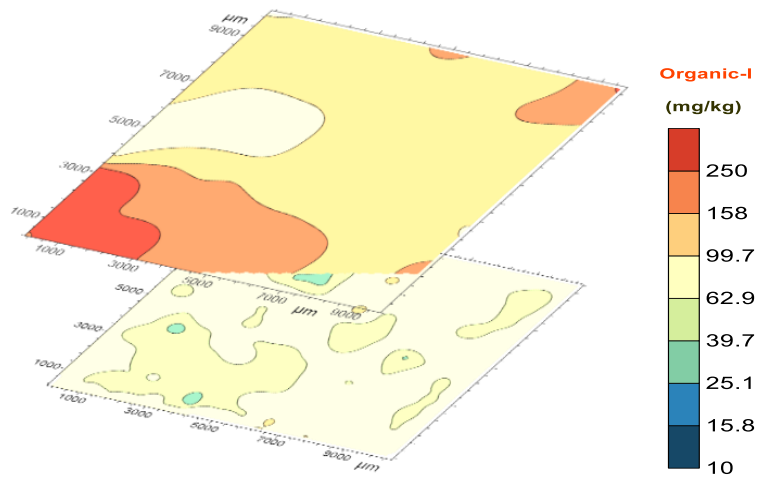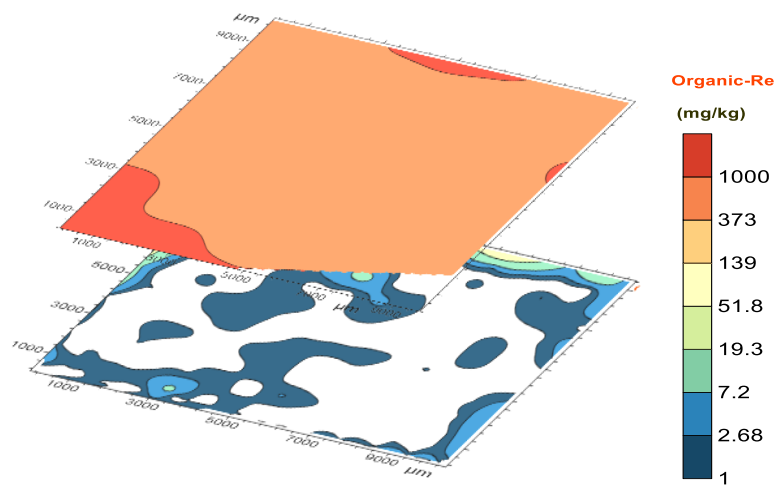
Chapter 5

Conclusion and Recommendation

Hydrocarbon production from unconventional shale reservoirs is still technically challenging, with shale wells experiencing rapid depletion rate and low recovery factor. The Utica Shale for instance, has a historical average first year decline of 65% percent (Jarvie, 2010). However, the root cause(s) of these trends have not been successfully understood. Using multiple complementary and innovative methods, this study looked into the pore structure (geometry and connectivity) of the Utica Shale region in a bid to understand low decline rate and overall low recovery in shale reservoirs.

The experimental methods used in investigating pore structure fluid movement in Utica Shale samples includes: mercury injection capillary pressure (MICP), imbibition, saturated diffusion and edge-only accessible porosity test from vacuum saturation and high-pressure tracer intrusion followed by LA-ICP-MS mapping of tracers. Results from MICP analyses shows that pore sizes of Utica Shale samples are predominantly in the nanometer size range across the study extent with a measured median pore-throat diameter of 9.5 nm, 9.2 nm, and 5.3 nm for J. Goins well at 940 feet, 973 feet and 1021 feet respectively. Prudential well has an average pore-throat diameter of 4.8 nm, 5.3 nm, and 4.8 nm at sample depth 1149 feet, 1293 feet and 1436 feet respectively. For Fred Barth well, median pore-throat diameter at depth 5647 feet, 5685 feet and 5746 feet are 4.2 nm, 5.5 nm, and 4.8 nm, respectively. Measured permeability for the study area was very low, with average values of 10.07 nD, 7.64 nD, and 0.65 nD for J. Goins, Prudential and Fred Barth wells, respectively. The small pore-size and low pore connectivity lead to anomalous imbibition behavior (which is consistent with percolation theory for tight shale rocks) as measured by imbibition experiment. Results from tracer imbibition and edge-only accessible porosity test reveals that pore connectivity in Utica Shale samples consistently

show that connected matrix pores seems only to be linked to a few mm from the sample edge followed with a random and sparse connection deeper into the samples. This poor connectivity and limited connected distance into shale matrix from sample edge will lead to steep initial decline and low overall production in the Utica Shale. This study can bridge the knowledge gap regarding the effects of nanopore connectivity and fluid flow in the Utica Shale play which would improve understanding of hydrocarbon molecules migration from the shale matrix to the stimulated fracture network and overall oil recovery.

Recommendation

While this study provides some level of enlightenment on pore geometry and connectivity and its effects on hydrocarbon production, more studies need to be conducted on fluid and tracers migration using advanced imaging techniques such as Micro and Macro CT, FIB-SEM and SANS to get better understanding of how hydrocarbon molecules migrate from shale matrix to the induced fracture network.

References

Abe, A.A. 2005. Relative Permeability and Wettability Implications of Dilute Surfactants at Reservoir Conditions. M.S. Thesis, Louisiana State University.

Bandy, R.E. 2012. Geology of the Eau Claire Formation and Conasauga Group in part of Kentucky and analysis of their suitability as caprocks for deeper CO_2 sequestration. M.S. Thesis, University of Kentucky.

Baihly, J., Altman, R., Malpani, R., Luo, F. 2011. Study assesses shale decline rates. The American Oil and Gas Reporter.

Banjade, Bharat. 2010. Subsurface Facies Analysis of the Cambrian Consauga Formation and Kerbel Formation in East-Central Ohio.

Black, D.F.B., Cressman, E.R., MacQuown, W.C., 1965. The Lexington Limestone (Middle Ordovician) of central Kentucky. U.S. Geological Survey Bulletin 1224-C, 29 p

Blakey, R. 2011. Paleogeography and Geologic Evolution of North America. Global Plate Tectonics and Paleogeography. Northern Arizona University.

Brett, C.E., McLaughlin, P.I., Cornell, S.R., Baird, G.C., 2004. Comparative sequence stratigraphy of two classic Uppeer Ordovician successions, Trenton Shelf (New York– Ontario) and Lexington Platform (Kentucky–Ohio): implications for eustasy and local tectonism in eastern Laurentia. Palaeogeogr. Palaeoclim. Palaeoecol. 210, 295–329.

Butterfield, A., 2014. Characterization of a Utica Shale Reflector Package Using Well Log Data and Amplitude Variation with Offset Analysis. M.S. Thesis, University of Mary Washington, 2011

Coogan, A.H. 1996. Ohio's surface rocks and sediments. In: Fossils of Ohio (R.M. Feldmann and M. Hackathorn, eds), pp. 31 – 50. Ohio Department of Natural Resources Division of Geological Survey, Columbus.

DeWitt, W.J. 1993. Principal of Oil and Gas Plays in the Appalachian Basin (Province 131). USGS Bulletin 1839-1

Dullien, F.A.L. 1992. Porous Media: Fluid Transport and Pore Structure (2nd Ed.). Academic Press, San Diego.

EIA (Energy Information Admistration). 2015. Drilling Productivity Report for Key Tight Oil and Shale Gas Regions. http://www.eia.gov/petroleum/drilling/pdf/dpr-full.pdf.

Ettensohn, F.R. 2008. The Appalachian Foreland Basin Eastern United States, *in* Miall, A., The sedimentary basins of United States and Canada: Sedimentary Basins of the World, Elsevier, Amsterdam, v.5, no. C, p. 105 – 179.

Ettensohn, F. R., and Brett, C. E., 2002, Stratigraphic evidence from the Appalachian Basin for continuation of the Taconian Orogenyinto Early Silurian time, in Mitchell, C. E. and Jacobi, R. eds., Taconic convergence: Orogen, foreland basin, and craton. Physics and Chemistry of the Earth, v. 27, pp. 279–288

EIA (Energy Information Administration), 2012. Annual Energy Outlook 2012: With Projections to 2035. U.S. Department of Energy, http://www.eia.gov/forecasts/AEO/.

Ewing, R.P., and R. Horton. 2002. Diffusion in sparsely connected pore spaces: Temporal and spatial scaling. *Water Resour. Res.*, 38: 1285, doi:10.1029/2002WR001412

Gao, Z.Y. and Q.H. Hu. 2013. Estimating permeability using median pore-throat radius obtained from mercury intrusion porosimetry. Journal of Geophysics and Engineering, v. 10, no. 2.

Hansen, Michael. 1997. The Geology of Ohio-The Ordovician: Ohio Geology, fall 1997.

Hill, D. G., Lombardi, T. E., Martin, J. P. 2002. Fractured Shale Gas Potential In New York: New York State Energy Research and Development Authority, 2002.

Hu, QH, Kneafsey, T.J, Trautz R.C, and Wang, JSY. 2004. Characterizing unsaturated diffusion in porous tuff gravels, Vadose zone Journal. 3(4): 1425-1438

Hu, Q.H., R.P. Ewing, and S. Dultz. 2012. Pore connectivity in Natural Rock. J. Contam. Hydrol, 133:76-83.

Hu, Q.H., and X.L. Mao. 2012. Applications of laser ablation inductively coupled plasma massSpectrometry in studying chemical diffusion, sorption, and transport in natural rock. Geochem. J., 46 (5):459–475.

Hu Q.H., Gao, X., Gao, Z., Ewing, R., Dultz, S., Kaufmann, J., 2014 Pore Accessibility and Connectivity of Mineral and Kerogen Phases in Shales. Unconventional Resources Technology Conference (URTeC)

Hu Q.H, Liu, X., Dultz, S., Ewing, R., Rowe, H.D. 2011. Fracture Matrix Interaction and Gas Recovery in the Barnett Shale. AAPG Search and Discovery Article #90122.

Huck, S.W. 2013. Controls on Natural Fractures in the Upper Lexington Limestone and Point Pleasant Formation: Central Ohio. M.S. Thesis, Bowling Green State University.

Hughes, J.D. 2013. Drill, Baby, Drill: Can Unconventional Fuels Usher in a New Era of Energy Abundance? Post Carbon Institute, 178 pp.

Hughes JD (2014) Drilling Deeper: A Reality Check on U.S. Government Forecasts for a Lasting Oil and Shale Gas Boom. Post Carbon Institute, 150 pp.

Hunt, A.G., R.P. Ewing, and B. Ghanbarian. 2014. Percolation Theory for Flow in Porous Media 3rd ed., Lect. Notes Phys. 880, Springer, Heidelberg.

Jarvie, D.M. 2010.Worldwide shale resource plays and potential. AAPG European Region ICE, October 17–19, 2010, Kiev, Ukraine.

Katz, A.J., and A.H. Thompson. 1986. A quantitative prediction of permeability in porous rock. Phys. Rev. B., 34: 8179–81.

Katz, A.J., and A.H. Thompson. 1987. Prediction of rock electrical conductivity from mercury injection measurements. *J. Geophy. Res.,* 92(B1): 599–607.

King, G.E. 2010. Thirty Years of Gas Shale Fracturing: What Have We Learned? SPE 133456

Kirschbaum, M.A., Schenk, C.J., Cook, T.A., Ryder, R.T., Charpentier, R.R., Klett, T.R., Gaswirth, S.B., Tennyson, M.E., Whidden, K.J. 2012. Assessment of undiscovered oil and gas resources of the Ordovician Utica Shale of the Appalachian Basin Province. U.S. Geological Survey Fact Sheet 2012; 3116:

Kuila, U., 2013. Measurement and Interpretation of Porosity and Pore-Size Distribution in Mudrocks: The Hole Story of Shales. Ph.D. Dissertation, Colorado School of Mines.

Liu, J.G., Nie, Y.F. 2001. Fractal scaling of effective diffusion coefficient of solute in porous media. Journal of Env. Sciences, China. Vol. 13 #2. Pp. 170 - 172

Lopez, R., Soria, A. 2007. Kinematical description of the spontaneous imbibition processes. IASME/WSEAS international conference, Athens, Greece.

Ma, S., N.R. Morrow, and X. Zhang. 1997. Generalized scaling of spontaneous imbibition data for strongly water-wet systems. J. Petrol. Sci. Eng., 18: 165–178.

Matyka, M., Koza, Z. 2012. How to calculate tortuosity easily? AIP Conference proceedings 1453, 17-22.

Maugeri, L. 2013. The shale oil boom: A U.S. phenomenon. Discussion Paper 2013-05, Belfer Center for Science and International Affairs, Harvard Kennedy School, June 2013.

Medina, C. Rupp, J., Avery, L.K., Venteris, E.R., Barnes, D.A., Harper, J.A., Greb, S., Slater, B.E.,Stolorow, A.,Sminchak, J. 2010, A regional characterization and assessment of geologic carbon sequestration opportunities in the upper Cambrian Mount Simon sandstone in the Midwest region: MRCSP Phase II Topical Report.

Micromeritics. 2001. Porosimetry brochure.

Monahan, P. D., 2014. Depositional Facies and Reservoir Analysis of the Tyler Formation in the Central Williston Basin, North Dakota. M.S. Thesis, University of Texas at Arlington.

Murphy, E., Warner, M., Sarmah, B. 2013. A workflow to Evaluate Porosity, Mineralogy, and TOC in the Utica-Point Pleasant Shale Play. SPE 165682

Pope, M.C., and Read, J.F., 1997, High-Resolution surface and subsurface sequence stratigraphy of the Middle to Late Ordovician (late Mohawkian– Cincinnatian) foreland basin rocks, Kentucky and Virginia: AAPG Bulletin 81, 1866–1893.

Olafuyi, O.A., Cinar, Y., Knackstedt, M. A., Pinczewski, W.V., 2007. Spontaneous Imbibition in Small Cores Bakken Shale. SPE 109724. Presented at the SPE Asia Pacific Oil &Gas Conference Oct. - Nov. 2007

Rowan, E.L. 2006. Burial and thermal history of the central Appalachian basin, based on three 2-D models of Ohio, Pennsylvania, and West Virginia: U.S. Geological Survey Open-File Report 2006-1019, 35 p.

Chaudhuri, B.R., Jessen, K., Tsotsis, T.T. 2010. Water inversion in shale: A preliminary Study. USC Viterbi Research Symposium.

Ryder, R.T. 1995. Appalachian Basin Province (067), *in* Gautier, D.L., Dolton, G.L., Takahashi, K.I., and Varnes, K.L., eds. National assessment of United States oil and gas resources – Results, methodology, and supporting data: U.S. Geological Survey Digital Data Series 30.

Ryder, R.T. 1992. Stratigraphic framework of Cambrian and Ordovician rocks in central Appalachian basin from Morrow County, Ohio, to Pendleton County, West Virginia. U.S. Geological Survey Bulletin, 1839.

Ryder, R.T. 2007. Assessment of Appalachian Basin Oil and Gas Resources: Utica-Lower Paleozoic Total Petroleum System. USGS Open File Report 2008-1287.

Riley, R.A., Baranoski, M.T., and Wickstrom, L.H., 2006, Regional stratigraphy of the Trenton-Black River, in Patchen, D.G., Hickman, J.B., Harris, D.C., Drahovzal, J.A., Lake, P.D., Smith, L.B., Nyahay, R., Schulze, R., Riley, R.A., Baranoski, M.T., Wickstrom, L.H., Laughrey, C.D., Kostelnik, J., Harper, J.A., Avary, K.L., Bocan, J., Hohn, M.E., and McDowell, R., A geologic play book for Trenton-Black River Appalachian basin exploration: U.S. Department of Energy Report, Morgantown, WV, DOE Award Number DE-FC26-03NT41856, p. 4-38, 30.

Paktinat, J., Pinkhouse, J.A., Fontaine, J. 2003. Investigation of methods to improve Utica hydraulic fracturing in the Appalachian basin. SPE 111063.

Patchen D., Hickman, J., Harris, D., Drahovzal, J., Lake, P., Smith, L., Nyahay, R., Schulze, R., Riley, R., Baranoski, M., Wickstrom, L., Laughrey, C., Kostelnik, J., Harper, J., Avary, K., Bocan, J., Hohn, M., McDowell, R. 2006. Geologic Play Book for Trenton-Black River Appalachian Exploration: Final Report. June 28, 2006.

Saeed. A., Evans, J.2012 Subsurface Facies Analysis of the Late Cambrian Mt. Simon Sandstone in Western Ohio (Midcontinent North America), *Open Journal of Geology*, Vol. 2 No. 2, 2012, p. 35-47

Swift, A., Sheets, J., Cole, D., Anovitz, L., Welch, S., Gu, X., Mildner, D., Chipera, S., Buchwalter, E., Cook, A. 2014. Nano- to microscale pore characterization of the Utica Shale. URTeC 1923522.

Thomas, A.R., Lendel, I., Hill, E.W., Southgate, D., Chase, R. 2012. An Analysis of the Economic Potential for Shale Formation in Ohio.

Wickstrom, L. 2013. Geology and activity of the Utica-Point Pleasant of Ohio. Search and Discovery Article #10490

Xie, X., and Morrow, N.R. 2001. Oil Recovery by Spontaneous Imbibition from Weakly Water-Wet Rocks. Petrophysics, Vol. 42, No. 4: 313- 322

Yu.w., and Sepehrnoori K. 2013. Stimulation of Gas Desorption and Geomechanics effects for Unconventional Gas Reserves. Elsevier, Fuel 166 (2014) 455-464.

Biographical Information

Francis Chukwuma was born on September 25th, 1987 in Benin CIty, Edo State, Nigeria. He is the fourth son of Sir O.F Chukwuma (KSJ) and Lady L.N Chukwuma. He received his Bachelor's Degree in Geology from University of Port Harcourt, Rivers States, Nigeria in 2010. He worked at Julius Berger Nigeria PLC, Voyager Oil and Gas Limited and Nigerian Geological Survey Agency where he gained hands-on experience in his field. He decided to pursue his Master's Degree in Petroleum Geosciences at University of Texas at Arlington. During his studying period at Arlington he developed a keen interest in Petrophysics and joined the CP3M research Group at UTA Geoscience department in January 2014 under the guidance of Dr. Q.H Hu. He attended numerous conferences and seminars on petrophysics, pore connectivity and fractures. After his graduation, he intends to find a job in energy field where he can use his knowledge and experience practically.